4. Okabe, Y., Kawane, K., Akira, S., Taniguchi, T. & Nagata, S. Toll-like receptor-independent gene induction program activated by mammalian DNA escaped from apoptotic DNA degradation. *J. Exp. Med.* **202**, 1333–1339 (2005).
5. Li, X. *et al.* Eya protein phosphatase activity regulates Six1–Dach–Eya transcriptional effects in mammalian organogenesis. *Nature* **426**, 247–254 (2003).
6. Rayapureddi, J. P. *et al.* Eyes absent represents a class of protein tyrosine phosphatases. *Nature* **426**, 295–298 (2003).
7. Tootle, T. L. *et al.* The transcription factor Eyes absent is a protein tyrosine phosphatase. *Nature* **426**, 299–302 (2003).
8. Akira, S., Uematsu, S. & Takeuchi, O. Pathogen recognition and innate immunity. *Cell* **124**, 783–801 (2006).
9. Medzhitov, R. Recognition of microorganisms and activation of the immune response. *Nature* **449**, 819–826 (2007).
10. Jemc, J. & Rebay, I. The eyes absent family of phosphotyrosine phosphatases: properties and roles in developmental regulation of transcription. *Annu. Rev. Biochem.* **76**, 513–538 (2007).
11. Kim, T. K. & Maniatis, T. The mechanism of transcriptional synergy of an *in vitro* assembled interferon-β enhanceosome. *Mol. Cell* **1**, 119–129 (1997).
12. Ohmori, Y. & Hamilton, T. A. Cooperative interaction between interferon (IFN) stimulus response element and κB sequence motifs controls IFNγ- and lipopolysaccharide-stimulated transcription from the murine IP-10 promoter. *J. Biol. Chem.* **268**, 6677–6688 (1993).
13. Sharma, S. *et al.* Triggering the interferon antiviral response through an IKK-related pathway. *Science* **300**, 1148–1151 (2003).
14. Iwamura, T. *et al.* Induction of IRF-3/-7 kinase and NF-κB in response to double-stranded RNA and virus infection: common and unique pathways. *Genes Cells* **6**, 375–388 (2001).
15. Kawai, T. *et al.* IPS-1, an adaptor triggering RIG-I- and Mda5-mediated type I interferon induction. *Nature Immunol.* **6**, 981–988 (2005).
16. Meylan, E. *et al.* Cardif is an adaptor protein in the RIG-I antiviral pathway and is targeted by hepatitis C virus. *Nature* **437**, 1167–1172 (2005).
17. Ohto, H. *et al.* Cooperation of six and eya in activation of their target genes through nuclear translocation of Eya. *Mol. Cell. Biol.* **19**, 6815–6824 (1999).
18. Ishikawa, H. & Barber, G. N. STING is an endoplasmic reticulum adaptor that facilitates innate immune signalling. *Nature* **455**, 674–678 (2008).
19. Moore, C. B. *et al.* NLRX1 is a regulator of mitochondrial antiviral immunity. *Nature* **451**, 573–577 (2008).
20. Tattoli, I. *et al.* NLRX1 is a mitochondrial NOD-like receptor that amplifies NF-κB and JNK pathways by inducing reactive oxygen species production. *EMBO Rep.* **9**, 293–300 (2008).
21. Jin, L. *et al.* MPYS, a novel membrane tetraspanner, is associated with major histocompatibility complex class II and mediates transduction of apoptotic signals. *Mol. Cell. Biol.* **28**, 5014–5026 (2008).
22. Cook, P. J. *et al.* Tyrosine dephosphorylation of H2AX modulates apoptosis and survival decisions. *Nature* **458**, 591–596 (2009).
23. Das, A. K., Helps, N. R., Cohen, P. T. & Barford, D. Crystal structure of the protein serine/threonine phosphatase 2C at 2.0 Å resolution. *EMBO J.* **15**, 6798–6809 (1996).
24. Lee, M. S. & Kim, Y. J. Signaling pathways downstream of pattern-recognition receptors and their cross talk. *Annu. Rev. Biochem.* **76**, 447–480 (2007).
25. Michallet, M. C. *et al.* TRADD protein is an essential component of the RIG-like helicase antiviral pathway. *Immunity* **28**, 651–661 (2008).
26. Abdelhak, S. *et al.* A human homologue of the *Drosophila* eyes absent gene underlies branchio-oto-renal (BOR) syndrome and identifies a novel gene family. *Nature Genet.* **15**, 157–164 (1997).
27. Orten, D. J. *et al.* Branchio-oto-renal syndrome (BOR): novel mutations in the EYA1 gene, and a review of the mutational genetics of BOR. *Hum. Mutat.* **29**, 537–544 (2008).
28. Mutsuddi, M. *et al.* Using *Drosophila* to decipher how mutations associated with human branchio-oto-renal syndrome and optical defects compromise the protein tyrosine phosphatase and transcriptional functions of eyes absent. *Genetics* **170**, 687–695 (2005).
29. Borsani, G. *et al.* EYA4, a novel vertebrate gene related to *Drosophila* eyes absent. *Hum. Mol. Genet.* **8**, 11–23 (1999).

Supplementary Information is linked to the online version of the paper at www.nature.com/nature.

Acknowledgements We thank T. Fujita and M. Yoneyama for the NDV, A. Sehara-Fujisawa for the myogenin promoter, and M. Fujii and M. Harayama for secretarial assistance. This work was supported in part by Grants-in-Aid from the Ministry of Education, Science, Sports, and Culture in Japan. T.S. is a Research Assistant for Kyoto University Global COE program (Center for Frontier Medicine).

Author Contributions Y.O. screened the cDNA library, and identified EYA4 as a regulator of the innate immune reaction. T.S. produced recombinant EYA in 293T cells and wheat-germ extracts, biochemically characterized, and found its threonine-phosphatase activity. S.N. designed the research and wrote the paper.

Author Information Reprints and permissions information is available at www.nature.com/reprints. Correspondence and requests for materials should be addressed to S.N. (snagata@mfour.med.kyoto-u.ac.jp).

METHODS

Cells, virus and other reagents. Monkey Vero cells were cultured in αMEM containing 15% FBS. MEFs and human 293T cells were cultured in DMEM containing 10% FBS. Human Namalwa cells were maintained in RPMI1640 containing 10% FBS. *DNase II*$^{-/-}$ MEFs expressing $\alpha_v\beta_3$-integrin (*DNase II*$^{-/-}$ MEFs/integrin) were described previously[4]. *DNase II*$^{-/-}$ *Irf3*$^{-/-}$ *Irf7*$^{-/-}$ MEFs were established from embryonic day (E)13.5 *DNase II*$^{-/-}$ *Irf3*$^{-/-}$ *Irf7*$^{-/-}$ mouse embryos as described[4]. To prepare the fetal liver macrophages, the liver from E14.5 mouse embryo was dissected and passed through a 22-gauge needle five times. After washing with PBS, the cells were cultured in αMEM containing 10% FBS supplemented with 10% (v/v) supernatant of CMG14-12 cells producing mouse macrophage colony-stimulating factor[30]. After 48 h, the cells were washed, and adherent cells were used as fetal liver macrophages. NDV was provided by T. Fujita (Kyoto University) and propagated in fertilized chicken eggs as described[31]. VSV (Indiana strain) was propagated in mouse L929 cells.

Antibodies used were mouse monoclonal antibodies against Flag (M2 antibody, Sigma), HA (clone 12C5, Boehringer Mannheim; clone 16B12, Babco), PARP (BD), and anti-tubulin (EMD Chemicals), rabbit polyclonal antibodies against IRF3 (Zymed Laboratories) and IPS-1 (Cell Signaling), and rabbit monoclonal antibody against phosphorylated-IRF3 (Ser 396; Cell Signaling).

Leucine zipper-tagged human Fas ligand[32] and mouse MFG-E8 (ref. 33) were produced in monkey COS7 and human 293T cells, respectively. Poly(I:C) was purchased from GE Healthcare. Calf thymus DNA, *E. coli* DNA and LPS were from Sigma. A phosphorothioate-stabilized CpG oligonucleotide[34] of 5′-TCCATGACGTTCCTGATGCT-3′ was purchased from Hokkaido System Science.

Production of monoclonal antibody against mouse EYA4. To produce monoclonal antibody against mouse EYA4, the N-terminal domain of EYA4 (amino acids 2–346) was joined to maltose-binding protein (MBP) using pMAL-p2X vector (New England BioLab), or to glutathione-*S*-transferase (GST) using pGEX-5X-1 vector (GE Healthcare). MBP–EYA4 and GST–EYA4 were produced in *E. coli* BL21(DE3) pLysS strain, and purified using Amylose-resin (New England BioLab) and glutathione-sepharose (GE Healthcare), respectively. Armenian hamsters were immunized by subcutaneously injecting four times with 50 μg of MBP–EYA4 in a 2-week interval. For the first injection, MBP–EYA4 was mixed with complete Freund's adjuvant (DIFCO), while it was mixed with incomplete Freund's adjuvant for the second to fourth injections. A final injection with 50 μg MBP-EYA4 was given into the foot pads. Two days later, popliteal and inguinal lymph nodes were collected, and the lymphocytes were fused with mouse myeloma NSO cell line[35]. Hybridomas were selected in HAT medium (Boehringer Ingelheim), and the supernatants were tested by ELISA for their ability to recognize GST–EYA4. Positive clones were examined for their suitability in western blotting, and one hybridoma (clone 5-7C 48) was subjected to limiting dilution. The hybridoma was grown in GIT medium (Nihon Pharmaceutical), and the antibodies were purified by protein A-sepharose.

Expression cloning. Poly(A) RNA was prepared from MEFs using an mRNA purification kit (GE Healthcare). Double-stranded cDNA was generated with the SuperScript Choice System (Invitrogen). cDNAs longer than 0.5 kb were ligated into a BstXI-digested pMXs vector[36] using the BstXI adaptor, and introduced into *E. coli* DH10B by electroporation, to generate a cDNA library of about 20,000 clones. The library was divided into 400 pools of 50 clones, and plasmid DNA was prepared from each pool using NucleoSpin Multi-96 Plus Plasmid (Macherey-Nagel). The DNA was introduced into Plat-E packaging cells[37], and the culture supernatant was used to infect *DNase II*$^{-/-}$ MEFs/integrin. At 48 h after the infection, the MEFs were allowed to engulf apoptotic *Cad*$^{-/-}$ thymocytes, and the concentration of CXCL10 in the culture supernatant was determined by ELISA. The pools that gave a positive result were subjected to sib-selection.

Engulfment of apoptotic cells and transfection of DNA. The MFG-E8-dependent engulfment of apoptotic cells was performed as described[33]. In brief, thymocytes from *Cad*$^{-/-}$ mice were treated for 2 h with Fas ligand to induce apoptosis in about 50% of the cell population. The apoptotic cells were added to MEFs at a ratio of 50:1, and incubated for 20 h in the presence of 0.1 μg ml^{-1} MFG-E8.

To introduce nucleic acids into cells, the nucleic acids were preincubated at room temperature for 15 min with FuGENE6 transfection reagent (Roche Diagnostics) at a ratio of 1:1.5 (w/v) in DMEM, added to the cells, and incubated at 37 °C for 6 (for macrophages) or 12 (for MEF and 293T) h.

Enzyme-linked immunosorbent assay. The concentrations of IFN-β and CXCL10 were determined by ELISAs using the mouse Interferon Beta ELISA Kit (PBL) and mouse CXCL10 DuoSet ELISA Development system (R&D), respectively. Streptavidin-conjugated horseradish peroxidase (HRP) or alkaline phosphatase was used as the substrate. In some cases, signals were amplified with the AmpliQ (Dako) detection system.

Real-time PCR. Total RNA was prepared from cells using the RNeasy kit with the RNase-Free DNase set (Qiagen). After reverse-transcription with oligo(dT) primer using a Transcriptor First Strand cDNA Synthesis Kit (Roche Diagnostics), aliquots of the products were amplified using the LightCycler 480 system (Roche Diagnostics) according to the instructions provided by the manufacturer. The primers used for the mouse genes were as follows: *Ifnb*, 5′-CCACCACAGCCCTCTCCATCAACTAT-3′ and 5′-CAAGTGGAGAGCAG TTGAGGACATC-3′; *Cxcl10*, 5′-CCATCAGCACCATGAACCCAAGT-3′ and 5′-CACTCCAGTTAAGGAGCCCTTTTAGACC-3′; β-actin, 5′-TGTGATGGT GGGAATGGGTCAG-3′, and 5′-TTTGATGTCACGCACGATTTCC-3′. The primers for the human genes were as follows: *IFNB*, 5′-CCAACAA GTGTCTCCTCCAAA-3′ and 5′-CCTCAGGGATGTCAAAGTTCA-3′; *EYA1*, 5′-AGGCACCATACAGCTACCAGAT-3′ and 5′-GCTGGTCATATAATGTGC TGGA-3′; *EYA2*, 5′-GGCACTAAACCTCATCAACTCC-3′ and 5′-CACCACG TAGACAGCTTTTCTG-3′; *EYA3*, 5′-CCAGATGTCAGTGATCAGAAGC-3′ and 5′-GGGTAGACAGCATAGGGTTGAG-3′; *EYA4*, 5′- CGCTTGTGTACGC TATTTGTTGT-3′ and 5′-TTTTCTCACTTCTCCTGCCACTC-3′; β-actin, 5′-GCATCCTCACCCTGAAGTAC-3′ and 5′-CTTAATGTCACGCACGATT TC-3′.

Expression plasmid. The cDNAs of mouse EYA1 (GenBank accession NP_034294), EYA2 (GenBank accession NP_034295), EYA3 (GenBank accession NP_034296), and EYA4 (GenBank accession NP_034297) were isolated by RT–PCR from the RNA of MEFs, and their authenticity was confirmed by DNA sequencing. As the N- and C-terminal regions of EYA3, amino acids 2–255 (encoded by exons 2–10), and amino acids 256–526 (encoded by exons 11–18), were used, respectively. Whereas amino acids 2–345 (encoded by exons 2–11), and amino acids 346–616 (encoded by exons 12–19), were used as the N- and C-terminal regions of EYA4, respectively. In the EYA4-Y4 mutant, tyrosine was replaced by alanine at four positions (amino acids 258, 261, 262 and 267). The EYA4-DYY mutant was produced by replacing Asn at position 246 and two Tyr residues at positions 247 and 250 with Ala. In the Asp352Asn mutant, the Asp at position 352 was replaced with Asn. The expression plasmid for these mutants were constructed by recombinant PCR[38]. All EYA proteins and their derivatives were Flag-tagged at the N terminus.

Mouse cDNAs for *Ips-1* (GenBank accession NP_659137), *Trif* (GenBank accession NP_778154), *Sting* (GenBank accession XP_905219), *Nlrx1* (GenBank accession NP_848507), *Irf3* (GenBank accession NP_058545), *Six4* (GenBank: NP_035512) and *MyD88* (GenBank: NP_034981) were isolated by RT–PCR from the RNA of MEF or fetal liver macrophages. Each cDNA was tagged with three tandem haemagglutinins (a peptide of influenza haemagglutinin, YPYDVPDYA) at the N terminus (IPS-1, TRIF, SIX4, NLRX1 and MyD88) or the C terminus (STING), or with Flag at the N terminus (IRF3).

Production of recombinant EYA proteins. The mouse EYA proteins were produced by transfecting human 293T cells with the respective expression plasmids, and the accumulated protein was purified using anti-Flag M2 affinity gel (Sigma). In brief, the expression vectors for Flag-tagged EYA and its derivatives were generated in pEF-BOS vector[39] and introduced into human 293T cells using the calcium-phosphate co-precipitation method. Sixty to seventy-two hours later, the cells were lysed by incubating them for 30 min at 4 °C in 50 mM Tris-HCl (pH 7.4) containing 1.0% (v/v) NP40, 150 mM NaCl, 2 mM EDTA, 2 mM EGTA, 2.0 μg ml^{-1} pepstatin, 2.0 μg ml^{-1} leupeptin, 2 μg ml^{-1} aprotinin, and 2 μM *p*ABSF (4-(2-aminoethyl)-benzenesulfonyl fluoride hydrochloride). After removing the cell debris by centrifugation at 39,800*g* for 40 min, the cell extracts were affinity-purified with anti-Flag-Sepharose (M2, Sigma), and the protein was eluted with 50 mM Tris-HCl buffer (pH 7.4) containing 100 μg ml^{-1} of Flag peptide (Sigma), 150 mM NaCl, and 0.1% NP40.

Recombinant EYA3 and EYA4 were also produced *in vitro* using the wheat-germ cell-free system[40]. In brief, the DNA fragment for the Flag-tagged EYA3 or EYA4 was inserted into pEU E01 vector (Cell Free Science). With the resultant plasmid as a template, *Eya3* or *Eya4* mRNA was synthesized with SP6 RNA polymerase using a kit from Cell Free Sciences according to the instructions provided by the manufacture. EYA protein was then synthesized with the mRNA by incubation at 15 °C for 20 h with 250 μl of wheat-germ extracts and 5.5 ml of SUM-AMIX (Cell Free Sciences). After incubation, the reaction mixture was diluted eightfold with 50 mM Tris-HCl (pH 7.4) containing 1.0% NP40, 150 mM NaCl, 2 mM EDTA, 2 mM EGTA, 2.0 μg ml^{-1} pepstatin, 2.0 μg ml^{-1} leupeptin, 2 μg ml^{-1} aprotinin and 2 μM *p*ABSF, and the Flag-tagged EYA protein was purified using anti-Flag-Sepharose as described earlier.

Assay for phosphatase activity. The phosphorylated synthetic peptides KR(pS)IRR, KR(pT)IRR, RRA(pT)VA and END(pY)INASL were custom-synthesized by the Toray Research Center, and KR(pT)IRR, DLDVPIPGRF DRRV(pT)VAAE, SDQEKRKQI(pT)VRGL, LDPRQVEMIRRRRP(pT)PAML, (pT)EEEEE, (pS)EEEEE, DADE(pY)LIPQQG, END(pY)INASL, RRLIEDAE (pY)AARG, TRDI(pY)ETDYYRK and DRV(pY)IHPF were custom-synthesized

by MBL. YSPTSPS(pY)SPTSPS, YSPTSPSY(pS)PT(pS)PS and YSPTSPSY SP(pT)SPS were custom-synthesized by Invitrogen. Sodium orthovanadate, okadaic acid and calyculin A were purchased from EMD Chemicals. Recombinant human protein phosphatase 2A, 2B and 2C were purchased from Wako, Promega and EMD Chemicals, respectively.

To assay the phosphatase activity, the recombinant EYA was incubated in a final volume of 50 μl with 400 μM phosphorylated peptide at 37 °C for 60 min in 50 mM MES-KOH buffer (pH 6.0) containing 2 mM $MgCl_2$ and 50 μM dithiothreitol (DTT) for the tyrosine phosphatase or in 50 mM Tricine-KOH buffer (pH 8.0) containing 5 mM EDTA and 50 μM DTT for the serine/threonine-phosphatase. The phosphatase activity of human protein phosphatase 2A, 2B and 2C was assayed similarly by incubating at 37 °C for 60 min. The buffer was essentially as previously reported[41,42]. That is, 50 mM Tris-HCl buffer (pH 7.0) containing 0.1 mM EGTA and 14.2 mM 2-mercaptoethanol for protein phosphatase 2A, 50 mM HEPES-KOH buffer (pH 7.5) containing 2 mM $NiCl_2$ for protein phosphatase 2B, and 50 mM Tris-HCl buffer (pH 7.5) containing 0.1 mM EDTA, 30 mM $MgCl_2$ and 1 mM DTT for protein phosphatase 2C. The released phosphate was quantified by a colourimetric method using the malachite green-molybdate as described[43]. In brief, the reaction was terminated by the addition of 50 μl of H_2O and 20 μl of 1.75% (w/v) ammonium molybdate·$4H_2O$ in 6.0 N H_2SO_4, and incubated at room temperature for 20 min. A solution (20 μl) containing 0.35% (w/v) malachite green and 0.35% (w/v) polyvinylalcohol (molecular mass 13,000–23000 Da) was added to the reaction mixture, which was further incubated for 20 min at room temperature. The malachite green-ammonium molybdate phosphate complex was detected at 620 nm using a Micro Plate Reader (BioLumin 960). K_m and K_{cat} values for the phosphatase activities of EYA were determined using Hanes-Woolf Plot.

Stable cell transformants. To express EYA and IRF3 in mouse MEFs and fetal liver macrophages, the corresponding cDNA was introduced into pMXs vector[36]. Retrovirus was prepared by transfecting PlatE packaging cells[37] with the expression vector, and used to infect MEF and macrophages[4]. To establish Namalwa cells that constitutively express mouse EYA4, the Flag-tagged EYA4 cDNA was introduced into pEF-BOS vector[39] to generate pEF-Flag-EYA4. Namalwa cells were co-transfected by electroporation with Aat II-digested pEF-Flag-EYA4 and a plasmid carrying the hygromycin-resistant gene. After being selected with 1.0 mg ml^{-1} hygromycin, the clones expressing EYA4 were identified by western blotting with anti-Flag antibody.

Cytopathic assay for VSV. Samples carrying VSV were seriously diluted, and incubated at 37 °C for 40 h with 1×10^4 Vero cells in 96-well microtitre plate. After incubation, surviving cells were stained with 0.5% crystal violet, and dissolved in methanol. Absorbance at 595 nm was determined using an ELISA reader (Infinite 2000, TECAN).

shRNA. shRNA expression plasmids for human *EYA1*, *EYA2*, *EYA3* and *EYA4* in a pRS shRNA vector carrying a puromycin-resistance gene were purchased from OriGene. The target sequences for the shRNAs were as follows: for human *EYA1*, 5′-ATCTGGCATCACCAGCCAAGCAGTTACAG-3′; for human *EYA2*, 5′-CC GAGTCACTTGCTGGTGAATACAACACA-3′; for human *EYA3*, 5′-AGT AGCCAGCATCTCAAACCAGGATTATC-3′; for human *EYA4*, 5′-CCTG AGGTTTGAATCTGACTTTAGCCTAC-3′; and for the control GFP, 5′-TGAC CACCCTGACCTACGGCGTGCAGTGC-3′. The U6-EYA1 and U6-EYA2 portions were joined into one pRS vector, and the U6-Eya3 and U6-EYA4 potions were joined into another pRS vector. Human 293T cells were transfected using the Fugene transfection reagent with the two shRNA plasmids. Sixty hours later, the cells were transfected with poly(I:C), and the *Ifnb* mRNA was quantified.

Luciferase assay. The promoter activity was determined by luciferase assay using the Dual-Luciferase Reporter Assay System (Promega). In brief, a DNA fragment carrying the mouse *Ifnb* promoter region (−121 to +22; +1, transcription start site)[44] was amplified by PCR from mouse genomic DNA. The mouse myogenin promoter (−182 to +52)[45] was provided by A. Sehara-Fujisawa (Kyoto University). The *Ifnb* and myogenin promoter was inserted upstream of the firefly luciferase gene of pGL3 to generate pGL3-mIFNβ125luc and pGL3MG-185, respectively. The expression vector for EYA4, IPS-1, TRIF, MyD88 or Six4 cDNA in pEF-BOS was introduced into MEF or 293T cells together with pGL3-mIFNβ125luc or pGL3MG-185 reporter plasmid. Twenty-four (for *Ifnb* promoter) or forty-eight (for myogenin promoter) hours later, the luciferase activity was determined as described previously[46]. pEF-Rluc or pSV-Rluc, which carries the *Renilla* luciferase gene downstream of the elongation factor 1 promoter[46] or SV40-early promoter, was used as an internal control for transfection.

Electrophoretic mobility shift assay. For the EMSAs, nuclear extracts were prepared as described[47]. The probe DNA carrying the NF-κB binding site (5′-AGTTGAGGGGACTTTCCCAGG-3′) was labelled with biotin using a biotin 3′ end DNA labelling kit (Pierce). For the binding reaction, nuclear extracts (2 μg protein) were incubated for 30 min at 25 °C with 20 fmol of biotin-labelled probe in 10 μl of a reaction mixture containing 10 mM Tris-HCl (pH 7.5), 50 mM KCl, 1 mM DTT, 5% glycerol, 2% polyvinylalcohol, and 500 ng poly(I:C) in the presence or absence of 4 pmoles of unlabelled probe. The reaction mixture was separated by electrophoresis on a 6% polyacrylamide gel in 50 mM Tris-HCl (pH 8.5) containing 380 mM glycine, and 2 mM EDTA, and the shifted band was detected with the LightShift Chemiluminescent EMSA Kit (Pierce).

Fractionation of the cell extracts. The cell extracts were fractionated into nuclear and cytoplasmic fractions as described previously[47]. In brief, MEFs were incubated at 4 °C for 10 min in hypotonic buffer (10 mM HEPES-KOH buffer (pH 7.9), 0.1 mM EDTA, 0.1 mM EGTA, 1 mM DTT, 10 mM KCl and a cocktail of protease inhibitors and phosphatase inhibitors (Roche Diagnostics) to allow cells to swell. The cells were then lysed by vigorously vortexing in the hypotonic buffer containing 6% sucrose and 0.1% NP-40. The lysates were spun at 14,000*g* for 2 min, and the supernatants were used as the cytoplasmic fraction. The pellets were suspended in 20 mM HEPES-KOH (pH 7.9) containing 0.2 mM EDTA, 2 mM EGTA, 2 mM DTT, 25% glycerol, 420 mM NaCl, and a cocktail of protease inhibitors and phosphatase inhibitors. After incubating at 4 °C for 30 min, the mixture was spun at 87,920*g* for 30 min, and the supernatants were used as nuclear extracts.

Immunoprecipitation and western blotting. Human 293T cells (2×10^6 cells) were transfected by the calcium-phosphate precipitation method with a total of 16 μg of expression plasmids for Flag-tagged or HA-tagged protein. Cells were collected 30 h after the transfection and lysed in lysis buffer containing 50 mM Tris-HCl (pH 8.0), 1% NP-40, 150 mM NaCl, 5 mM EDTA, and a cocktail of protease inhibitors and phosphatase inhibitors (Roche Diagnostics). Cell lysates were precleared by incubating at 4 °C with Sepharose CL-4B (Sigma) for 2 h, and then incubated with anti-Flag M2 affinity gel for 2 h. After washing with the lysis buffer, the proteins bound to the beads were eluted by boiling in SDS sample buffer (62.5 mM Tris-HCl (pH 6.8), 2% SDS, 10% glycerol, 5% 2-mercaptoethanol, and 0.001% bromphenol blue), separated by electrophoresis on a 10% or 10–20% polyacrylamide gel, and transferred onto a PVDF membrane. The membrane was incubated with biotin-conjugated mouse anti-Flag, or mouse anti-HA (clone 12CA5), followed by incubation with HRP-conjugated streptavidin (Roche Diagnostics). The peroxidase activity was detected by Immobilon Western ECL system (Millipore). In some case, cells were lysed with SDS sample buffer, and directly subjected to SDS–PAGE, followed by western blotting.

For analysis by native PAGE[14], cells were suspended in 50 mM Tris-HCl (pH 7.5) containing 150 mM NaCl, 1 mM EDTA, 2% NP-40, cocktails of protease inhibitors and phosphatase inhibitors (Roche Diagnostics). After being briefly vortexed, the mixture was spun for 10 min at 17,600*g*, and the supernatant (3 μg protein) was separated by electrophoresis at 20 mA on a 7.5% polyacrylamide gel (Bio-Rad) in 62.5 mM Tris-HCl buffer (pH 6.8) containing 15% glycerol and 1% deoxycholate, and transferred to a PVDF membrane for western blotting analysis.

30. Takeshita, S., Kaji, K. & Kudo, A. Identification and characterization of the new osteoclast progenitor with macrophage phenotypes being able to differentiate into mature osteoclasts. *J. Bone Miner. Res.* **15**, 1477–1488 (2000).
31. Lam, K. M. & Hao, Q. Induction of lymphocyte agglutination and lysis by Newcastle disease virus. *Vet. Microbiol.* **15**, 49–56 (1987).
32. Shiraishi, T. *et al.* Increased cytotoxicity of soluble Fas ligand by fusing isoleucine zipper motif. *Biochem. Biophys. Res. Commun.* **322**, 197–202 (2004).
33. Hanayama, R. *et al.* Identification of a factor that links apoptotic cells to phagocytes. *Nature* **417**, 182–187 (2002).
34. Hemmi, H. *et al.* A Toll-like receptor recognizes bacterial DNA. *Nature* **408**, 740–745 (2000).
35. Ray, S. & Diamond, B. Generation of a fusion partner to sample the repertoire of splenic B cells destined for apoptosis. *Proc. Natl Acad. Sci. USA* **91**, 5548–5551 (1994).
36. Kitamura, T. *et al.* Retrovirus-mediated gene transfer and expression cloning: powerful tools in functional genomics. *Exp. Hematol.* **31**, 1007–1014 (2003).
37. Morita, S., Kojima, T. & Kitamura, T. Plat-E: an efficient and stable system for transient packaging of retroviruses. *Gene Ther.* **7**, 1063–1066 (2000).
38. Higuchi, R. in *PCR Protocols: a Guide to Methods and Applications* 177–188 (Academic, 1990).
39. Mizushima, S. & Nagata, S. pEF-BOS, a powerful mammalian expression vector. *Nucleic Acids Res.* **18**, 5322 (1990).
40. Sawasaki, T., Ogasawara, T., Morishita, R. & Endo, Y. A cell-free protein synthesis system for high-throughput proteomics. *Proc. Natl Acad. Sci. USA* **99**, 14652–14657 (2002).
41. Donella Deana, A. *et al.* An investigation of the substrate specificity of protein phosphatase 2C using synthetic peptide substrates; comparison with protein phosphatase 2A. *Biochim. Biophys. Acta* **1051**, 199–202 (1990).
42. Umeda, I. O., Nakata, H. & Nishigori, H. Identification of protein phosphatase 2C and confirmation of other protein phosphatases in the ocular lenses. *Exp. Eye Res.* **79**, 385–392 (2004).
43. Van Veldhoven, P. P. & Mannaerts, G. P. Inorganic and organic phosphate measurements in the nanomolar range. *Anal. Biochem.* **161**, 45–48 (1987).
44. Yoneyama, M. *et al.* Direct triggering of the type I interferon system by virus infection: activation of a transcription factor complex containing IRF-3 and CBP/p300. *EMBO J.* **17**, 1087–1095 (1998).

45. Fujisawa-Sehara, A., Hanaoka, K., Hayasaka, M., Hiromasa-Yagami, T. & Nabeshima, Y. Upstream region of the myogenin gene confers transcriptional activation in muscle cell lineages during mouse embryogenesis. *Biochem. Biophys. Res. Commun.* **191**, 351–356 (1993).
46. Kawane, K. *et al.* Structure and promoter analysis of murine CAD and ICAD genes. *Cell Death Differ.* **6**, 745–752 (1999).
47. Shapiro, D. J., Sharp, P. A., Wahli, W. W. & Keller, M. J. A high-efficiency HeLa cell nuclear transcription extract. *DNA* **7**, 47–55 (1988).

blood

2009 113: 1332-1339
Prepublished online Nov 20, 2008;
doi:10.1182/blood-2008-07-167148

Lactadherin and clearance of platelet-derived microvesicles

Swapan K. Dasgupta, Hanan Abdel-Monem, Polly Niravath, Anhquyen Le, Ricardo V. Bellera, Kimberly Langlois, Shigekazu Nagata, Rolando E. Rumbaut and Perumal Thiagarajan

Blood (print ISSN 0006-4971, online ISSN 1528-0020), is published semimonthly by the American Society of Hematology, 1900 M St, NW, Suite 200, Washington DC 20036.

Lactadherin and clearance of platelet-derived microvesicles

*Swapan K. Dasgupta,[1,2] *Hanan Abdel-Monem,[1,2] Polly Niravath,[3] Anhquyen Le,[1,2] Ricardo V. Bellera,[4] Kimberly Langlois,[4] Shigekazu Nagata,[5] Rolando E. Rumbaut,[1,2,4] and Perumal Thiagarajan[1-3]

[1]Michael E. DeBakey VA Medical Center, Houston, TX; Departments of [2]Pathology, [3]Medicine, and [4]Pediatrics, Baylor College of Medicine, Houston, TX; and [5]Department of Genetics, Osaka University Medical School, Osaka, Japan

The transbilayer movement of phosphatidylserine from the inner to the outer leaflet of the membrane bilayer during platelet activation is associated with the release of procoagulant phosphatidylserine-rich small membrane vesicles called platelet-derived microvesicles. We tested the effect of lactadherin, which promotes the phagocytosis of phosphatidylserine-expressing lymphocytes and red blood cells, in the clearance of platelet microvesicles. Platelet-derived microvesicles were labeled with BODIPY-maleimide and incubated with THP-1–derived macrophages. The extent of phagocytosis was quantified by flow cytometry. Lactadherin promoted phagocytosis in a concentration-dependent manner with a half-maximal effect at approximately 5 ng/mL. Lactadherin-deficient mice had increased number of platelet-derived microvesicles in their plasma compared with their wild-type littermates (950 ± 165 vs 4760 ± 650; $P = .02$) and generated 2-fold more thrombin. In addition, splenic macrophages from lactadherin-deficient mice showed decreased capacity to phagocytose platelet-derived microvesicles. In an in vivo model of light/dye-induced endothelial injury/thrombosis in the cremasteric venules, lactadherin-deficient mice had significantly shorter time for occlusion compared with their wild-type littermate controls (5.93 ± 0.43 minutes vs 9.80 ± 1.14 minutes; $P = .01$). These studies show that lactadherin mediates the clearance of phosphatidylserine-expressing platelet-derived microvesicles from the circulation and that a defective clearance can induce a hypercoagulable state. (Blood. 2009;113:1332-1339)

Introduction

In platelets, as in most mammalian cells, anionic phospholipids such as phosphatidylserine are present only in the inner leaflet of the membrane bilayer.[1] During platelet activation, phosphatidylserine moves from the inner to the outer leaflet of the membrane bilayer.[2] The transbilayer movement of phosphatidylserine is responsible for platelet procoagulant activity by providing high-affinity binding sites for the assembly of the prothrombinase and tenase complex.[3,4] Externalization of anionic phospholipids in platelets is accompanied by the release of phosphatidylserine-rich microvesicles.[5,6] These microvesicles are procoagulant and account for the clot-promoting activity of the serum.[7] More recently, in addition to their hemostatic role, platelet-derived microvesicles were shown to stimulate hematopoietic cells[8] and to transfer platelet-specific receptors to the surface of other cells.[9]

Lactadherin, also known as milk fat globule–epidermal growth factor 8 (EGF-8), is a 45-kDa glycoprotein secreted by macrophages.[10,11] Lactadherin contains EGF-like domains at the amino terminus and 2 C-domains at the carboxy terminus that share homology to the phosphatidylserine-binding domains of blood coagulation factors V and VIII.[12,13] Lactadherin binds to apoptotic cells, activated platelets, and phosphatidylserine-expressing red blood cells via the C-domains and anchors them to macrophage integrins via its RGD sequence in the EGF domain.[14-17] We have examined the role of lactadherin in the clearance of phosphatidylserine-rich platelet-derived microvesicles.

Methods

Reagents

Lactadherin was isolated from fresh unhomogenized milk and labeled with fluorescein isothiocyanate (FITC) as described previously.[18] Annexin A5 was isolated as described previously.[19] The carboxy-terminal fragment of human lactadherin (C1C2 fragment) was amplified from a lactadherin cDNA using primers 5′-TTGAATTCCAGTACGTGAGATTGTACCCCACG-3′ and 5′-TTTGCGGCCGCTAACAGCCCAGCAGCTCC-3′. The amplified fragments were digested with *Eco*R1 and *Not*1 and ligated to the bacterial expression vector pET-28. The recombinant fragment was isolated from *Escherichia coli* as described for bovine lactadherin fragment.[20] Generation of monoclonal antibody to lactadherin was previously described.[21] BODIPY (4,4-difluoro-4-bora-3a,4a-diaza-s-indacene)–maleimide was purchased from Invitrogen (Carlsbad, CA). Human thrombin and purified Russell viper venom were purchased from Haematologic Technologies (Essex Junction, VT). Collagen was purchased from Helena Laboratories (Beaumont, TX). Phycoerythrin (PE)–labeled monoclonal anti–human platelet glycoprotein Ib (anti-CD42b) was purchased from Beckman Coulter (Fullerton, CA). PE-labeled murine anti-CD42b antibody was obtained from eBioscience (San Diego, CA).

Mice

All animal protocols were approved by the Institutional Animal Care and Use Committee of Baylor College of Medicine. C57BL/6J mice were purchased from The Jackson Laboratory (Bar Harbor, ME). The generation of lactadherin-deficient mice was described previously.[22] The lactadherin$^{-/-}$ mice were rederived at Baylor College of Medicine in C57BL/6 mice and backcrossed 6 times to C57BL/6 background.

Submitted July 8, 2008; accepted November 5, 2008. Prepublished online as *Blood* First Edition paper, November 20, 2008; DOI 10.1182/blood-2008-07-167148.

The publication costs of this article were defrayed in part by page charge payment. Therefore, and solely to indicate this fact, this article is hereby marked "advertisement" in accordance with 18 USC section 1734.

*S.K.D. and H.A.-M. contributed equally to this study.

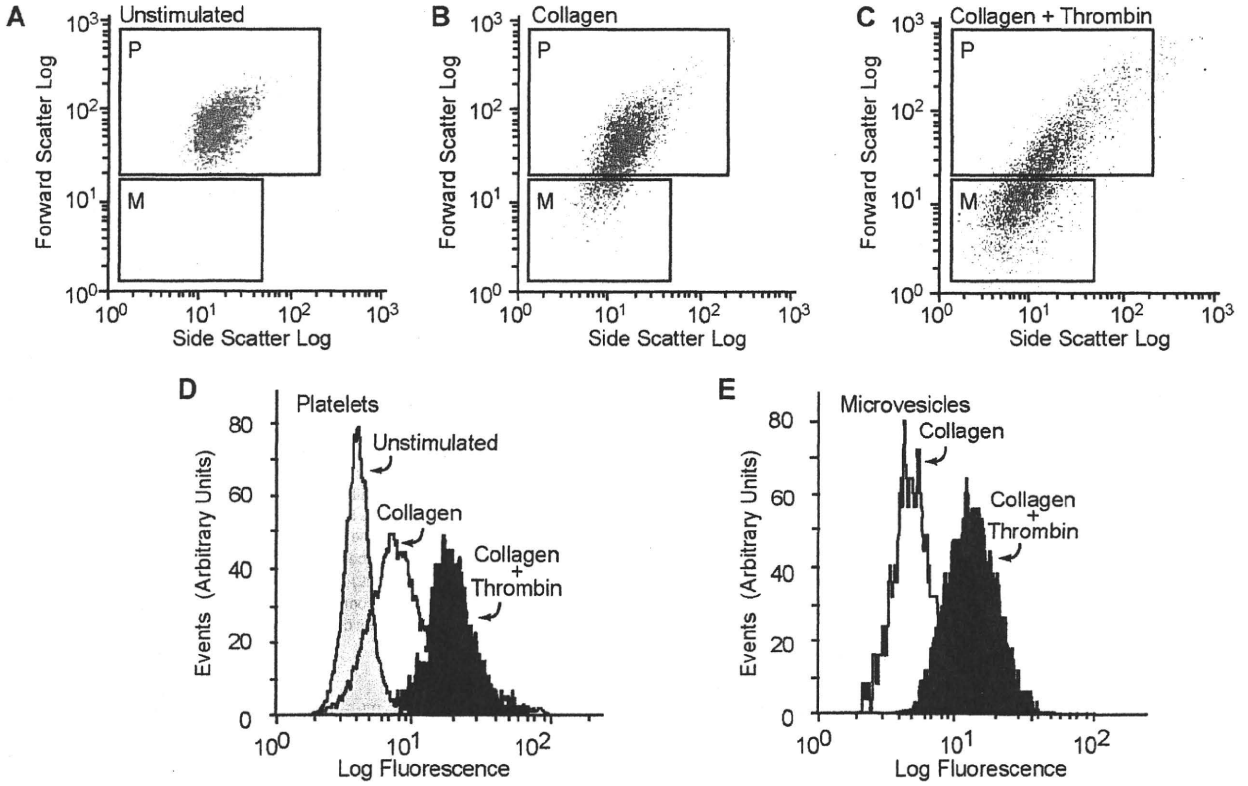

Figure 1. Lactadherin binding to platelets and platelet-derived microvesicles. Washed human platelets were treated with (A) buffer only, (B) collagen (50 μg/mL), or (C) a combination of thrombin (0.1 U/mL) and collagen (50 μg/mL), and FITC-lactadherin (5 μg/mL) and a PE-labeled anti-CD42b (2.5 μg/mL) were added. The generation of microvesicles was analyzed by flow cytometry as described before.[6] To resolve the platelets and platelet-derived microparticles from background scatter, only $CD42b^+$ events were analyzed for forward and side scattering. The gates for microvesicles (gate M) and intact platelets (gate P) were set with the use of isolated microvesicles and unstimulated platelets, respectively. Platelets and microvesicles were analyzed separately for the expression of phosphatidylserine by 5 μg/mL FITC-lactadherin (D,E).

Flow cytometric analysis of lactadherin binding to platelets and platelet-derived microvesicles

Washed platelets were prepared from healthy volunteers after informed consent was obtained in accordance with the Declaration of Helsinki and approved by the Committee for Protection of Human Subjects at Baylor College of Medicine, as described before.[18] Platelets were resuspended in a modified Tyrode buffer[18] containing 1% bovine serum albumin and 1 mM $CaCl_2$. They were activated with collagen (50 μg/mL) or a combination of thrombin (0.1 U/mL) and collagen (50 μg/mL) for 20 minutes at room temperature. FITC-lactadherin (5 μg/mL) and a PE-labeled anti-CD42b (2.5 μg/mL) were added and incubated for 30 minutes at room temperature. Aliquots were then analyzed on a flow cytometer (Coulter FCC 500; Beckman Coulter) using the CXP software. The gates for microvesicles and intact platelets were set with the use of isolated microvesicles and unstimulated platelets, respectively. To differentiate platelets and platelet-derived microvesicles from background scatter, $CD42b^+$ events were gated and analyzed for forward and side scattering. The light scatter and fluorescence channels were set at a logarithmic gain (Figure 1). Ten thousand events per sample were acquired to ensure adequate mean fluorescence levels.

Detection of platelet microvesicle-associated lactadherin in normal human plasma

Blood was drawn through 19-gauge needles into polypropylene syringes containing a one-tenth volume of 3.8% trisodium citrate, pH 6.5. The blood was immediately transferred to polypropylene tubes, and the platelet-rich plasma (PRP) was obtained by centrifugation at 1000*g* for 3 minutes at room temperature. The PRP was centrifuged at 5000*g* for 15 minutes at 4°C to obtain platelet-poor plasma (PPP). The PPP was further centrifuged at 20 000*g* for 20 minutes to sediment the microvesicles. The pellet containing microvesicles was suspended in the modified Tyrode buffer for further analysis. The microvesicles were incubated with a PE-labeled anti-CD42b (2.5 μg/mL) and FITC-anti–lactadherin antibody, L688 (5 μg/mL) for 30 minutes at room temperature for flow cytometry.

Detection of microvesicle-bound lactadherin

An aliquot (100 μg in 100 μL) of rabbit polyclonal anti-IIb/IIIa antibody[23] or irrelevant rabbit control antibody was incubated overnight at 4°C with 100 μL Protein A+G agarose beads (Santa Cruz Biotechnology, Santa Cruz, CA) and washed 3 times (10 000*g* for 2 minutes) in HEPES-buffered saline (HBS). The washed beads were incubated overnight at 4°C with 5 mL human PPP, centrifuged, and washed 3 times in HBS. Bound proteins were eluted in 50 μL 1% SDS and centrifuged and subjected to sodium dodecyl sulfate–polyacrylamide gel electrophoresis (SDS-PAGE; 10%), transferred to a PVDF membrane. The blot was incubated with a monoclonal antibody to lactadherin, L688,[17] and developed with a peroxidase-labeled goat anti–mouse antibody (Thermo Scientific, Rockford, IL) using 4-chloro-1-naphthol (0.3 mg/mL) and H_2O_2 (0.03%).

Isolation and labeling of microvesicles

Washed human platelets were incubated with a combination of thrombin (0.1 U/mL) and collagen (50 μg/mL) for 30 minutes and centrifuged at 2000*g* for 15 minutes. The supernatant plasma, which is platelet-free and microvesicle-rich (as determined by flow cytometry), was further centrifuged at 20 000*g* for 20 minutes. The pellet containing microvesicles was resuspended in HBS and incubated with BODIPY-maleimide (2.5 μM) for 20 minutes and washed twice by centrifugation at 20 000*g* for 20 minutes in HBS.

Peripheral blood mononuclear cells were isolated as described previously,[24] and an aliquot of mononuclear cells (10^8/mL) was stimulated with calcium ionophore A23187 (10 μM) for 30 minutes at 37°C with gentle stirring. The cell suspension was centrifuged at 5000*g* for 15 minutes, the pellet was discarded, and the microvesicles were isolated by centrifugation at 20 000*g* for 20 minutes and labeled with BODIPY-maleimide as described for platelet-derived microvesicles. Human umbilical vein endothelial cells were detached with trypsin-EDTA, washed in serum-free tissue-culture medium (RPMI 1640), and stimulated with calcium ionophore A23187 (10 μM) for 30 minutes at 37°C to release microvesicles. The microvesicles were isolated by centrifugation and labeled as described earlier for human platelet-derived microvesicles.

To isolate microvesicles from mouse platelets, blood was drawn in EDTA (5 mM final concentration) from 4-month-old mice under isoflurane anesthesia from the inferior vena cava and diluted with an equal volume of HBS. PRP was obtained by centrifugation at 260*g* for 10 minutes. Prostaglandin E1 (1 μM) was added, and platelets were sedimented by centrifugation at 1000*g* for 10 minutes and washed twice in modified Tyrode buffer as described for human platelets. Platelet suspension was stimulated with calcium ionophore A23187 (10 μM) containing 1.5 mM $CaCl_2$ at 37°C for 1 hour. The suspension was centrifuged at 5000*g* for 10 minutes, and the pellet was discarded. The microvesicles were labeled with BODIPY-maleimide as described earlier. Splenic macrophages were isolated as described before.[24]

Quantitation of microvesicles from mouse blood

Microvesicles in mouse plasma were quantified as described before with some modification.[25] Briefly, mouse PRP was centrifuged at 5000*g* for 10 minutes at room temperature, and the PPP (250 μL) was diluted to 1 mL by adding 750 μL HBS and incubated with PE-labeled anti–mouse CD42b and analyzed by flow cytometry. The microvesicles were gated as described before for human microvesicles. The flow rate was kept at 10 μL/minute and was run for exactly 3 minutes. On the basis of the dilution, rate, and the time of flow, we calculated the number of microvesicles per microliter of plasma.

Phagocytosis assay

Phagocytosis of platelet-derived microvesicles was quantified by the method described by Hoffmeister et al[26] with some modifications. THP-1 cells (ATCC, Manassas, VA) were grown in tissue culture medium (RPMI 1640 containing 10% fetal bovine serum). The cells were washed in serum-free medium, and phorbol 12-myristate 13-acetate (150 ng/mL) was added and plated on 12-well tissue-culture dish (10^6 cells/well) coated with 2% poly 2-hydroxyethyl methacrylate and incubated for 15 minutes at 37°C. BODIPY-labeled microvesicles (~80 μg) were added to the cells and incubated at 37°C for 30 minutes in the presence of various concentrations of lactadherin. THP-1 cells were incubated with 0.05% trypsin-EDTA to promote detachment and to remove any surface-bound platelet-derived microvesicles. The trypsin was neutralized with fetal calf serum, and the cells were washed twice in serum-free medium and incubated with a PE-labeled anti-CD11b monoclonal antibody (5 μg/mL). The THP-1 cells were gated based on PE fluorescence and forward light scatter and were analyzed for BODIPY fluorescence (green). The results were presented as the percentage of green (BODIPY) fluorescence-positive macrophages. The basal level of phagocytosis, in absence of lactadherin, varied from 10% to 25%.

Thrombin generation assay

Blood samples were collected from mice after anesthesia with a "clean" puncture of the inferior vena cava one-tenth volume of 3.8% trisodium citrate, pH 6.5. Blood samples from 5 mice from each group (lactadherin$^{-/-}$ and littermate controls [lactadherin$^{+/+}$]) were pooled, and PRP was obtained by centrifugation at 260*g* for 10 minutes. PPP was obtained from PRP by centrifuging the blood at 5000*g* for 10 minutes. Microvesicle-free plasma was obtained by further centrifuging the plasma at 20 000*g* for 20 minutes. Thrombin generation in plasma was measured as described before.[27] Briefly, each plasma sample (80 μL) was combined with trigger solution (40 μL) consisting of purified Russell viper venom (3 ng), fluorogenic thrombin substrate Z-Gly-Gly-Arg-AMC (2.5 mM), and $CaCl_2$ (10 mM). The generation of thrombin was measured as a function of fluorescence measured on a fluorimeter over 30 minutes. Thrombin was then quantified by the method described by Hemker et al[27] with the use of an α_2-macroglobulin thrombin complex as standard.

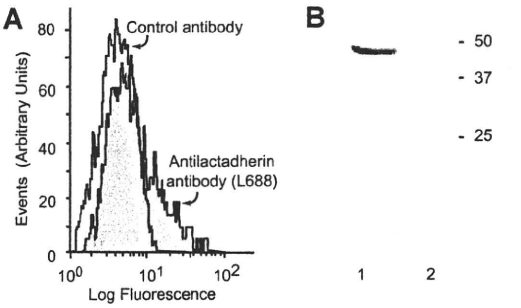

Figure 2. Lactadherin is present in circulating platelet-derived microvesicles in normal human plasma. (A) Microvesicles, isolated from normal human plasma by centrifugation, were incubated with PE-labeled anti-CD42b (2.5 μg/mL) and FITC-antilactadherin antibody L688 (5 μg/mL) or an FITC-labeled irrelevant control antibody. The CD42b-expressing particles were gated and analyzed for FITC fluorescence. (B) Immunoblot of microvesicle-associated lactadherin. Protein A + G agarose beads (100 μL) were incubated overnight at 4°C with 100 μg rabbit polyclonal anti-IIb/IIIa antibody or an irrelevant rabbit control antibody. The beads were washed and incubated with 5 mL platelet-poor plasma and washed. Bound proteins were eluted in 50 μL 1% SDS, subjected to SDS-PAGE, transferred to PVDF membrane, and probed with the monoclonal antibody to lactadherin L688[29] and developed by a peroxidase-labeled goat anti–mouse antibody (1/2000 dilution) and chloronaphthol (0.3 mg/mL) and H_2O_2 (0.03%). (Lane 1) Anti-IIb/IIIa antibody and (lane 2) irrelevant control antibody. (Lane 1) Immunoprecipitation with anti-IIb/IIIa and (lane 2) irrelevant control antibody.

Splenectomy in mice

Mice (4 months old) were anesthetized with an inhalation of isoflurane for the duration of the surgery. After a midline laparotomy, the small bowel was moved to the right of the abdominal cavity and covered with sterile saline. The spleen was approached by dissection, and the splenic blood vessels were tied with Vicryl sutures, and the spleen was removed. The laparotomy was closed in 2 layers with sutures. Four hours later, blood sample was obtained from the inferior vena cava as described earlier.

Mouse model of thrombosis

The in vivo thrombosis was assessed in a mouse model of light/dye-induced endothelial injury as described previously.[28] Mice were anesthetized with an intraperitoneal injection of pentobarbital sodium (50 mg/kg), with additional doses (12.5 mg/kg) as needed. The mice were then placed on a custom Plexiglas tray and maintained at 37°C with a homeothermic blanket and a rectal temperature probe (FHC, Bowdoinham, ME). A tracheotomy was performed to facilitate breathing, and an internal jugular vein and common carotid artery were cannulated for intravenous drug administration and blood pressure/heart rate monitoring, respectively. The cremaster microvascular bed was prepared as described[28] and was superfused continuously with a pH-equilibrated (pH range, 7.35-7.45) bicarbonate-buffered saline solution at 35°C. The preparation was then transferred to the stage of an upright intravital videomicroscope (BX-50; Olympus, Tokyo, Japan) and allowed to equilibrate for 30 minutes. A 4× objective (NA 0.13) lens was used to survey the vascular bed, and a 40× water-immersion objective (NA 0.8) was used to monitor thrombosis kinetics. After a 30-minute equilibration period on the microscope stage, 10 mL/kg 5% FITC-labeled dextran (150 kD) was injected intravenously through the jugular vein. A suitable venule with brisk flow and minimal leukocyte adhesion was selected. After measuring the diameter and blood flow velocity of the vessel

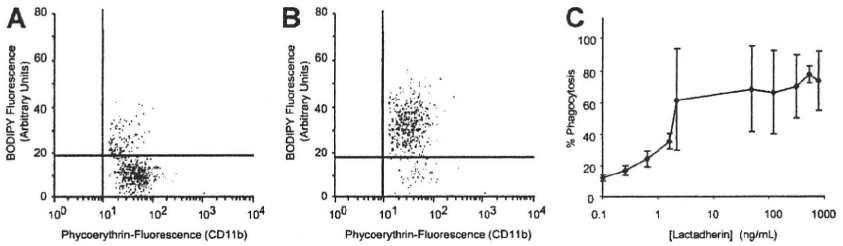

Figure 3. Phagocytosis of platelet-derived microvesicles by macrophages. BODIPY-maleimide–labeled human platelet-derived microvesicles (80 μg) were incubated with THP-1–derived macrophages (10^6 cells/well) for 30 minutes. The nonadherent and the surface-bound microvesicles were detached with trypsin-EDTA solution. The macrophages were washed and analyzed by flow cytometry. The macrophages were identified by PE-labeled CD11b and gated. Phagocytosis was quantified by measuring the percentage of BODIPY (green) fluorescence-positive macrophages. (A) Phagocytosis in the absence of lactadherin. (B) Phagocytosis in the presence of lactadherin (0.8 μg/mL). (C) Lactadherin concentration-dependent phagocytosis of microvesicles. Each point represents the mean and SD of 3 or more separate experiments.

(Doppler velocimeter; Microcirculation Research Institute, College Station, TX), a photochemical injury was started by exposing approximately 100 μm of the vessel to filtered excitation light at 0.6 W/cm² (from a 175W xenon lamp; Sutter Instrument, Novato, CA; and an HQ-FITC filter cube; Chroma Technology, Brattleboro, VT).[28,29] Epi-illumination was applied continuously, and the time of onset of platelet aggregates (thrombus onset) and the time of flow cessation (for at least 60 seconds) were recorded. Typically, thrombi were induced in 2 venules per animal, and the results for each animal were averaged.

Statistical analysis

All data are expressed as means and standard deviations of triplicate measurements except when indicated otherwise. Comparisons between individual groups were performed with the use of the Student *t* test with paired and unpaired samples. A probability value (*P*) of .05 or less was considered statistically significant.

Results

Phosphatidylserine expression on platelet microvesicles

Resting washed platelet suspensions had few microparticles (Figure 1A). After activation with collagen, or with a combination of collagen and thrombin, a distinct subpopulation of microvesicles was seen with different light-scattering characteristics (Figure 1A-C) as described before.[6] The expression of phosphatidylserine was measured by FITC-lactadherin binding. FITC-lactadherin binding was increased both in platelets and in microparticle fractions after activation (Figure 1D,E).

Lactadherin is bound to circulating platelet-microvesicles

In normal plasma, platelet-derived microvesicles constitute a major fraction of circulating microvesicles. Because lactadherin is also present in normal plasma,[30] the circulating platelet-derived microvesicles were examined for the presence of lactadherin. Lactadherin is present on the outer surface of platelet-derived microvesicles, as determined by flow cytometry, using a monoclonal antibody to lactadherin L688 (Figure 2A). Lactadherin was also shown in immunoblots of platelet microvesicles, isolated by immunoabsorption with agarose-bound anti–glycoprotein IIb/IIIa antibodies (Figure 2B).

Lactadherin promotes the phagocytosis of microvesicles by macrophages

Differentiated human monocytic THP-1 cells have been used as an in vitro model for phagocytic clearance.[26] When THP-1–derived macrophages were incubated with BODIPY-labeled platelet-derived microvesicles, approximately 10% to 25% of macrophages had phagocytosed platelet-derived microvesicles (Figure 3A). Lactadherin promoted phagocytosis in a concentration-dependent manner with half-maximal effect at approximately 5 ng/mL (Figure

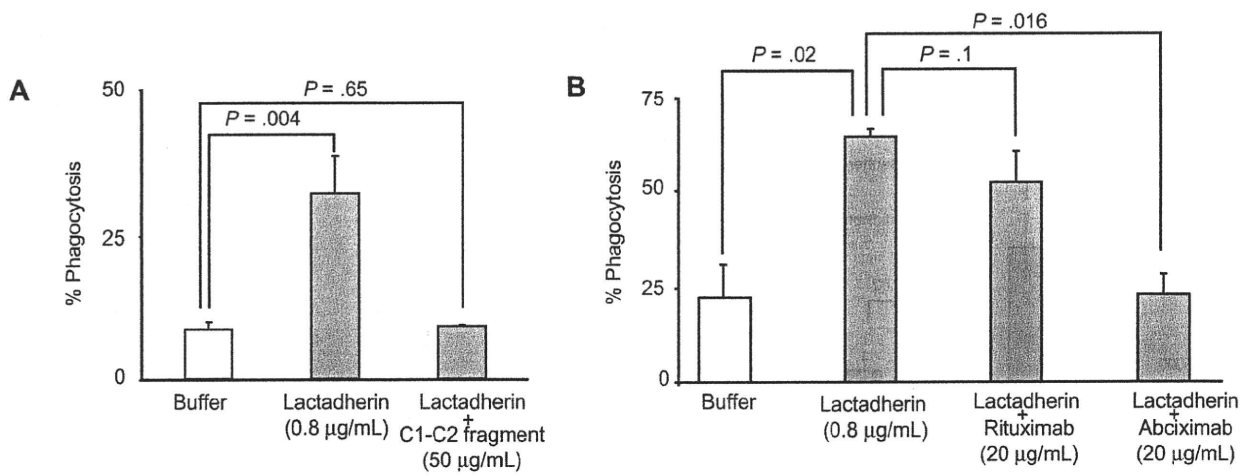

Figure 4. Inhibition of lactadherin-dependent phagocytosis of platelet-derived microvesicles. (A) THP-1–derived macrophages were incubated with BODIPY-labeled human platelet-derived microvesicles and lactadherin in the presence of C1C2 fragment (A) or abciximab (B). The extent of phagocytosis was measured as described in Figure 3. The results are the means and SDs of triplicate measurements.

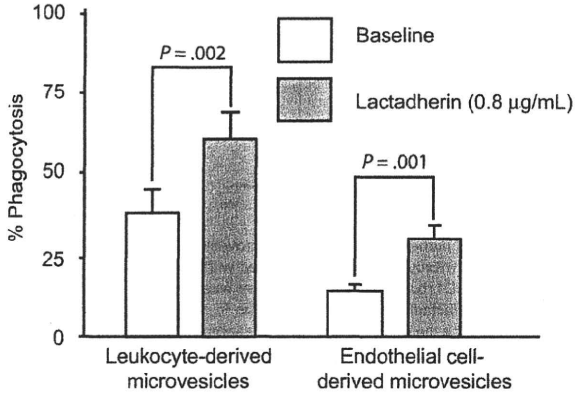

Figure 5. Effect of lactadherin on the phagocytosis of leukocytes and endothelial cell–derived microvesicles. BODIPY-maleimide–labeled microvesicles from peripheral blood leukocytes or human umbilical vein endothelial cells were incubated with THP-1–derived macrophages (10^6 cells/well) for 30 minutes with or without lactadherin (0.8 μg/mL), and the extent of phagocytosis was quantified by flow cytometry by measuring the percentage of green fluorescence (BODIPY)–positive macrophages as in Figure 3.

3B,C). The carboxy-terminal fragment of lactadherin, which has only the phosphatidylserine binding domain (but not the integrin binding domain), inhibited lactadherin-dependent phagocytosis of platelet-derived microvesicles (Figure 4A). Because lactadherin-dependent phagocytosis is mediated by integrins,[10] we examined the effect of abciximab, a human-mouse hybrid Fab fragment that reacts with integrin β3. Abciximab inhibited lactadherin-dependent phagocytosis to approximately 50%, whereas under similar conditions an irrelevant control antibody had no effect (Figure 4B). The stimulatory effect of lactadherin was also seen for the phagocytosis of leukocyte and endothelial cell–derived microvesicles (Figure 5).

Lactadherin-deficient mice have increased microvesicles in the circulation

To determine whether the in vitro findings have an in vivo significance, we quantified the microvesicles in lactadherin-deficient mice and the wild-type littermates by flow cytometry. Littermate control mice had on, an average, 4257 (± 700) microvesicles/μL of blood (Figure 6). In contrast, lactadherin-deficient mice had 8940 (± 1035) microvesicles/μL ($P = .02$; Figure 6). The platelet-derived microvesicles (as determined by CD42b expression) were increased 5-fold in the lactadherin-deficient mice compared with littermate controls (950 ± 165 vs 4760 ± 650; $P = .02$). We posit that the difference is due to the impaired clearance of phosphatidylserine-expressing microvesicles.

Lactadherin-deficient mice have defective phagocytosis of phosphatidylserine-expressing microvesicles

We further studied the phagocytosis of platelet-derived microvesicles by the splenic macrophages isolated from lactadherin-deficient mice and their littermate controls. The splenic macrophages from lactadherin-deficient mice had decreased phagocytosis of phosphatidylserine-expressing microvesicles compared with the wild-type littermate control macrophages (Figure 7; $P = .006$; n = 3). Addition of exogenous lactadherin to lactadherin-deficient macrophages corrected the defect in phagocytosis (Figure 7).

Lactadherin-deficient mice generate significantly more thrombin compared with wild-type littermate controls

To determine whether the increased presence of microvesicles in the plasma of lactadherin-deficient mice is associated with increased procoagulant activity, we measured thrombin generation in their plasma. Plasma from lactadherin-deficient mice generated twice as much thrombin as did their wild-type littermate controls (41.5 nM vs 20.4 nM in 30 min) under similar conditions (Figure 8). The difference between the lactadherin-deficient mice and their wild-type littermates was not present in the supernatant plasma, from which microvesicles had been removed by ultracentrifugation.

Hypercoagulable state in lactadherin-deficient mice

Because microvesicles are increased in lactadherin-deficient mice, and plasma from lactadherin-deficient mice generates more thrombin, we tested in vivo thrombus formation in a light/dye-induced endothelial injury/thrombosis model in cremasteric venules. No significant difference was observed in the initiation time for thrombus formation (0.53 ± 0.07 min vs 0.65 ± 0.17 min; $P = .46$; n = 9 in each group) between lactadherin-deficient mice and their wild-type littermate controls (lactadherin$^{+/+}$). However, in lactadherin-deficient mice the time for occlusion was significantly shorter (5.93 ± 0.43 min vs 9.80 ± 1.14 min; $P = .01$; n = 9 in each group; Figure 9). Microvascular diameters and wall shear rates did not differ between lactadherin-deficient mice and littermate controls (44.3 ± 1.0 μm vs 44.8 ± 1.3 μm, and 513.7 ± 29.8 sec^{-1} vs 550.6 ± 54.0 sec^{-1}, respectively).

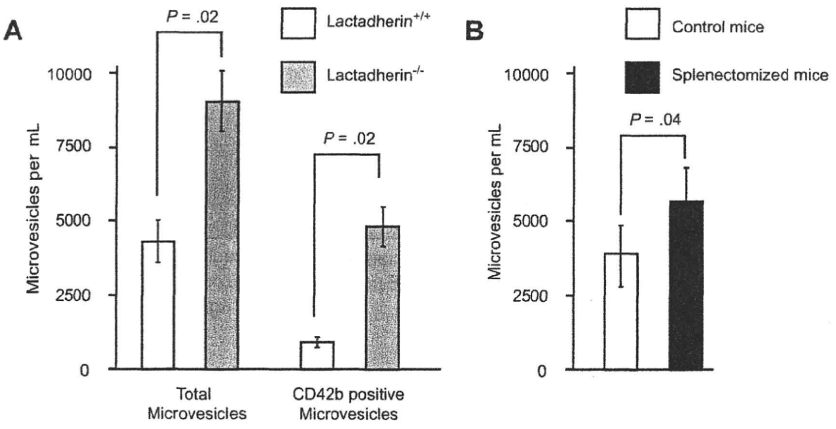

Figure 6. Circulating microvesicles in mouse blood. (A) Plasma was collected from lactadherin-deficient mice and their littermate controls (N = 3 for each group). The microvesicles were quantified by flow cytometry, based on the light scatter and surface expression of CD42b (n = 3). (B) Wild-type mice were subjected to splenectomy, and the circulating microvesicles were measured 4 hours later. The results are the means and SDs (N = 3).

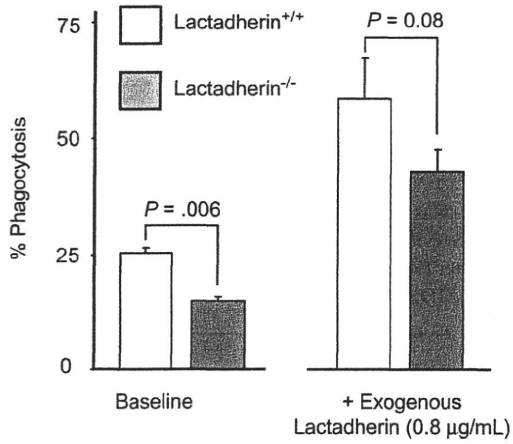

Figure 7. Phagocytosis of platelet-derived microvesicles by splenic macrophages in mice. Splenic macrophages were isolated from lactadherin-deficient mice and their wild-type littermate controls and incubated with BODIPY-labeled mouse platelet-derived microvesicles in the absence or presence of exogenous lactadherin. Phagocytosis of microvesicles was quantified as described before. The results are the means and SDs of triplicate measurements.

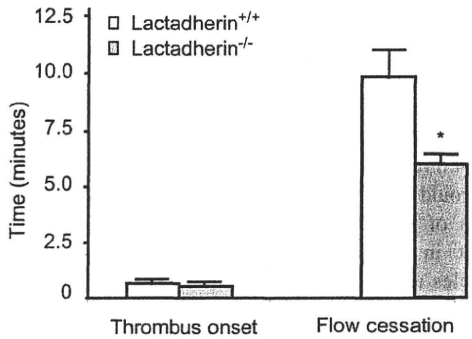

Figure 9. Thrombus formation in lactadherin-deficient mice. Endothelial injury was induced by light/dye in vivo in the cremasteric venules. Thrombus onset and flow cessation were monitored by intravital microscopy in lactadherin-deficient mice (▩) and the littermate controls (□). *$P = .01$; $n = 9$.

Similarly, heart rate and blood pressure did not differ statistically between lactadherin-deficient mice and controls (440.6 ± 24.4 beats/min vs 453.3 ± 15.1 beats/min, and 76.8 ± 4.0 mm Hg vs 68.2 ± 2.2 mm Hg, respectively).

Discussion

The clearance of apoptotic cells by phagocytes is an extremely efficient process. However, even in tissues that are known to contain a large fraction of cells undergoing apoptosis (such as the bone marrow), it is difficult to detect apoptosis by traditional methods, because the apoptotic cells are engulfed rapidly by macrophages.[31] The exposure of phosphatidylserine that occurs during apoptosis is the best-studied macrophage recognition signal, and several receptors have been identified in macrophages that mediate apoptotic cell clearance by binding to phosphatidylserine on apoptotic cells directly or indirectly.[32]

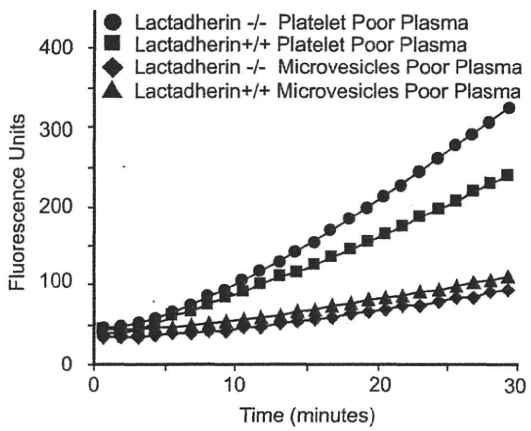

Figure 8. Thrombin generation in the plasma of lactadherin-deficient mice and control littermates. The reaction mixture consisted of plasma (80 μL) and the trigger solution (3 ng purified Russell viper venom in 40 μL), fluorogenic thrombin substrate Z-Gly-Gly-Arg-AMC (2.5 mM), and $CaCl_2$ (10 mM). The generation of thrombin was measured as a function of fluorescence in a fluorimeter over a period of 30 minutes. Thrombin was then calculated using an α_2-macroglobulin thrombin complex standard as described by Hemker et al.[27] Representative data are presented. Blood samples from 5 mice from each group (lactadherin$^{-/-}$ and littermate controls [lactadherin$^{+/+}$]) were pooled for each experiment.

Platelets lack the machinery to undergo the type of programmed cell death of nucleated cells. However, they appear to have a similar pathway of clearance when activated, involving exposure of phosphatidylserine. Phosphatidylserine is normally located on the cytoplasmic face of the resting platelet membrane. However, after platelet activation with certain agonists that induce sustained increase in intraplatelet calcium such as collagen and shear stress, phosphatidylserine appears on the plasma-oriented surface.[2,4] Externalization of phosphatidylserine in platelet is accompanied by the release of phosphatidylserine-rich microvesicles that are derived from the surface blebs of activated platelets.[6] These microvesicles, initially described as "platelet dusts," are responsible for the clot-promoting activity of plasma.[7] In addition to providing an efficient catalytic surface for prothrombin and factor X activation, microvesicles may have additional hemostatic effects. Microvesicles localize to the subendothelium after vessel wall injury,[33] providing sites for adhesion of platelets and neutrophils.[34] They also improve hemostasis in hemophilic mice.[35] Microvesiculation is defective in Scott syndrome, an inherited bleeding disorder with impaired platelet procoagulant activity resulting from the failure to externalize phosphatidylserine after platelet activation.[36]

Our results show that lactadherin, a macrophage opsonin that mediates the clearance of apoptotic lymphocytes, is one of the mediators of the clearance of phosphatidylserine-expressing procoagulant platelet-derived microvesicles. Platelet-derived microvesicles have a short half-life of less than 5 minutes[37] and must be continuously formed. In an enzyme-linked immunoabsorbent assay assay, we detected approximately 19 plus or minus 1 ng/mL in normal plasma. After centrifugation at 20 000*g* for 20 minutes, the level decreased to 10 plus or minus 4 ng/mL, suggesting at least 25% of the plasma lactadherin is bound to microvesicles. Lactadherin-deficient mice have increased concentration of microvesicles at steady state, presumably because of their defective clearance, leading to a procoagulant state. The defective phagocytosis by the splenic macrophages from the lactadherin-deficient mice is corrected by exogenous lactadherin. Furthermore, complement-dependent phagocytosis of

zymosan-coated fluorescent particles is normal in lactadherin-deficient mice,[24] indicating no global defect in macrophage function.

Lactadherin competes efficiently with factor V and factor VIII for binding sites on phosphatidylserine with a half-maximal effect at 1 to 4 nM.[38] The procoagulant state seen in lactadherin deficiency could also be due to the absence of natural anticoagulant function of lactadherin. However, increased thrombin is not apparent in microvesicle-poor plasma, suggesting that microvesicles are responsible for the increased thrombin generation. The clearance of phosphatidylserine-containing apoptotic cell surfaces is a fundamental process in development and tissue repair. Therefore, it is not surprising that multiple redundant receptors are involved in their clearance.[31] These receptors are also probably involved in the clearance of platelet-derived microvesicles.

Plasma levels of platelet-derived microvesicles are increased in cancer-associated deep vein thrombosis,[39] antiphospholipid antibody syndrome,[40] disseminated intravascular coagulation, heparin-induced thrombocytopenia,[41] and thrombotic thrombocytopenic purpura,[42] all conditions associated with either arterial and venous thrombosis. The procoagulant microvesicles may have a role in the hypercoagulable state in these conditions. Furthermore, defective clearance of apoptotic cell surfaces is a prominent pathogenetic mechanism in human and murine lupus, and the defective clearance of these vesicles may also play a role in the hypercoagulable state seen in these disorders.

Acknowledgments

This work was supported by grants from the Veterans Affairs Research Service (Washington, DC), the Gulf Coast Regional Blood Center (Houston, TX), and the National Institutes of Health (Bethesda, MD; HL-079368).

Authorship

Contribution: R.E.R. and P.T. designed the experiments; P.N. performed the thrombin generation assay; A.L. cultured the cells and generated the antibodies; R.V.B. and K.L. performed the mouse thrombosis assay; S.N. provided the lactadherin-deficient mice; and S.K.D. and H.A.-M. performed the protein isolation and phagocytosis assay.

Conflict-of-interest disclosure: The authors declare no competing financial interests.

Correspondence: Perumal Thiagarajan, Michael E. DeBakey VA Medical Center, Mail Stop #113, 2002 Holcombe Boulevard, Houston, TX 77030; e-mail perumalt@bcm.tmc.edu.

References

1. Zwaal RF, Comfurius P, Bevers EM. Surface exposure of phosphatidylserine in pathological cells. Cell Mol Life Sci. 2005;62:971-988.
2. Bevers EM, Comfurius P, Zwaal RF. Regulatory mechanisms in maintenance and modulation of transmembrane lipid asymmetry: pathophysiological implications. Lupus. 1996;5:480-487.
3. Zwaal RF, Schroit AJ. Pathophysiologic implications of membrane phospholipid asymmetry in blood cells. Blood. 1997;89:1121-1132.
4. Solum NO. Procoagulant expression in platelets and defects leading to clinical disorders. Arterioscler Thromb Vasc Biol. 1999;19:2841-2846.
5. Comfurius P, Senden JM, Tilly RH, Schroit AJ, Bevers EM, Zwaal RF. Loss of membrane phospholipid asymmetry in platelets and red cells may be associated with calcium-induced shedding of plasma membrane and inhibition of aminophospholipid translocase. Biochim Biophys Acta. 1990;1026:153-160.
6. Sims PJ, Wiedmer T, Esmon CT, Weiss HJ, Shattil SJ. Assembly of the platelet prothrombinase complex is linked to vesiculation of the platelet plasma membrane. Studies in Scott syndrome: an isolated defect in platelet procoagulant activity. J Biol Chem. 1989;264:17049-17057.
7. Wolf P. The nature and significance of platelet products in human plasma. Br J Haematol. 1967; 13:269-288.
8. Baj-Krzyworzeka M, Majka M, Pratico D, et al. Platelet-derived microparticles stimulate proliferation, survival, adhesion, and chemotaxis of hematopoietic cells. Exp Hematol. 2002;30:450-459.
9. Rozmyslowicz T, Majka M, Kijowski J, et al. Platelet- and megakaryocyte-derived microparticles transfer CXCR4 receptor to CXCR4-null cells and make them susceptible to infection by X4-HIV. AIDS. 2003;17:33-42.
10. Hanayama R, Tanaka M, Miwa K, Shinohara A, Iwamatsu A, Nagata S. Identification of a factor that links apoptotic cells to phagocytes. Nature. 2002;417:182-187.
11. Akakura S, Singh S, Spataro M, et al. The opsonin MFG-E8 is a ligand for the alphavbeta5 integrin and triggers DOCK180-dependent Rac1 activation for the phagocytosis of apoptotic cells. Exp Cell Res. 2004;292:403-416.
12. Hvarregaard J, Andersen MH, Berglund L, Rasmussen JT, Petersen TE. Characterization of glycoprotein PAS-6/7 from membranes of bovine milk fat globules. Eur J Biochem. 1996;240:628-636.
13. Andersen MH, Graversen H, Fedosov SN, Petersen TE, Rasmussen JT. Functional analyses of two cellular binding domains of bovine lactadherin. Biochemistry. 2000;39:6200-6206.
14. Asano K, Miwa M, Miwa K, et al. Masking of phosphatidylserine inhibits apoptotic cell engulfment and induces autoantibody production in mice. J Exp Med. 2004;200:459-467.
15. Shi J, Pipe SW, Rasmussen JT, Heegaard CW, Gilbert GE. Lactadherin blocks thrombosis and hemostasis in vivo: correlation with platelet phosphatidylserine exposure. J Thromb Haemost. 2008;6:1167-1174.
16. Shi J, Shi Y, Waehrens LN, Rasmussen JT, Heegaard CW, Gilbert GE. Lactadherin detects early phosphatidylserine exposure on immortalized leukemia cells undergoing programmed cell death. Cytometry A. 2006;69:1193-1201.
17. Dasgupta SK, Thiagarajan P. The role of lactadherin in the phagocytosis of phosphatidylserine-expressing sickle red blood cells by macrophages. Haematologica. 2005;90:1267-1268.
18. Dasgupta SK, Guchhait P, Thiagarajan P. Lactadherin binding and phosphatidylserine expression on cell surface-comparison with annexin A5. Transl Res. 2006;148:19-25.
19. Thiagarajan P, Benedict CR. Inhibition of arterial thrombosis by recombinant annexin V in a rabbit carotid artery injury model. Circulation. 1997;96: 2339-2347.
20. Shao C, Novakovic VA, Head JF, Seaton BA, Gilbert GE. Crystal structure of lactadherin C2 domain at 1.7 angstrom resolution with mutational and computational analyses of its membrane-binding motif. J Biol Chem. 2007;283: 7230-7241.
21. Guchhait P, Dasgupta SK, Le A, Yellapragada S, Lopez JA, Thiagarajan P. Lactadherin mediates sickle cell adhesion to vascular endothelial cells in flowing blood. Haematologica. 2007;92:1266-1267.
22. Hanayama R, Tanaka M, Miyasaka K, et al. Autoimmune disease and impaired uptake of apoptotic cells in MFG-E8-deficient mice. Science. 2004; 304:1147-1150.
23. Thiagarajan P, Shapiro SS, Levine E, DeMarco L, Yalcin A. A monoclonal antibody to human platelet glycoprotein IIIa detects a related protein in cultured human endothelial cells. J Clin Invest. 1985;75:896-901.
24. Dasgupta SK, Abdel-Monem H, Guchhait P, Nagata S, Thiagarajan P. Role of lactadherin in the clearance of phosphatidylserine-expressing red blood cells. Transfusion. 2008;48:2370-2374.
25. Dale GL, Remenyi G, Friese P. Quantitation of microparticles released from coated-platelets. J Thromb Haemost. 2005;3:2081-2088.
26. Hoffmeister KM, Felbinger TW, Falet H, et al. The clearance mechanism of chilled blood platelets. Cell. 2003;112:87-97.
27. Hemker HC, Giesen P, Al Dieri R, et al. Calibrated automated thrombin generation measurement in clotting plasma. Pathophysiol Haemost Thromb. 2003;33:4-15.
28. Rumbaut RE, Randhawa JK, Smith CW, Burns AR. Mouse cremaster venules are predisposed to light/dye-induced thrombosis independent of wall shear rate, CD18, ICAM-1, or P-selectin. Microcirculation. 2004;11:239-247.
29. Rumbaut RE, Sial AJ. Differential phototoxicity of fluorescent dye-labeled albumin conjugates. Microcirculation. 1999;6:205-213.
30. Yamaguchi H, Takagi J, Miyamae T, et al. Milk fat globule EGF factor 8 in the serum of human patients of systemic lupus erythematosus. J Leukoc Biol. 2008;83:1300-1307.
31. Ravichandran KS, Lorenz U. Engulfment of apoptotic cells: signals for a good meal. Nat Rev Immunol. 2007;7:964-974.
32. Fadok VA, Bratton DL, Henson PM. Phagocyte

receptors for apoptotic cells: recognition, uptake, and consequences. J Clin Invest. 2001;108:957-962.

33. Merten M, Pakala R, Thiagarajan P, Benedict CR. Platelet microparticles promote platelet interaction with subendothelial matrix in a glycoprotein IIb/IIIa-dependent mechanism. Circulation. 1999; 99:2577-2582.
34. Forlow SB, McEver RP, Nollert MU. Leukocyte-leukocyte interactions mediated by platelet microparticles under flow. Blood. 2000;95:1317-1323.
35. Hrachovinova I, Cambien B, Hafezi-Moghadam A, et al. Interaction of P-selectin and PSGL-1 generates microparticles that correct hemostasis in a mouse model of hemophilia A. Nat Med. 2003;9:1020-1025.
36. Zwaal RF, Comfurius P, Bevers EM. Scott syndrome, a bleeding disorder caused by defective scrambling of membrane phospholipids. Biochim Biophys Acta. 2004;1636:119-128.
37. Rand ML, Wang H, Bang KW, Packham MA, Freedman J. Rapid clearance of procoagulant platelet-derived microparticles from the circulation of rabbits. J Thromb Haemost. 2006;4: 1621-1623.
38. Shi J, Gilbert GE. Lactadherin inhibits enzyme complexes of blood coagulation by competing for phospholipid-binding sites. Blood. 2003;101: 2628-2636.
39. Tesselaar ME, Romijn FP, Van Der Linden IK, Prins FA, Bertina RM, Osanto S. Microparticle-associated tissue factor activity: a link between cancer and thrombosis? J Thromb Haemost. 2007;5:520-527.
40. Combes V, Simon AC, Grau GE, et al. In vitro generation of endothelial microparticles and possible prothrombotic activity in patients with lupus anticoagulant. J Clin Invest. 1999;104:93-102.
41. Lee DH, Warkentin TE, Denomme GA, Hayward CP, Kelton JG. A diagnostic test for heparin-induced thrombocytopenia: detection of platelet microparticles using flow cytometry. Br J Haematol. 1996;95:724-731.
42. Kelton JG, Warkentin TE, Hayward CP, Murphy WG, Moore JC. Calpain activity in patients with thrombotic thrombocytopenic purpura is associated with platelet microparticles. Blood. 1992;80: 2246-2251.

Cell PRESS

Immunity

The Many Roles of FAS Receptor Signaling in the Immune System

Andreas Strasser,[1,*] Philipp J. Jost,[1] and Shigekazu Nagata[2,*]
[1]The Walter and Eliza Hall Institute of Medical Research, Melbourne, VIC 3050, Australia
[2]Graduate School of Medicine, Kyoto University, Kyoto 606-8501, Japan
*Correspondence: strasser@wehi.edu.au (A.S.), snagata@mfour.med.kyoto-u.ac.jp (S.N.)
DOI 10.1016/j.immuni.2009.01.001

FAS belongs to the subgroup of the tumor necrosis factor receptor (TNF-R) family that contains an intracellular "death domain" and triggers apoptosis. Its physiological ligand FASL is a member of the TNF cytokine family. Studies with mutant mice and cells from human patients have shown that FAS plays critical roles in the immune system, including the killing of pathogen-infected cells and the death of obsolete and potentially dangerous lymphocytes. Fas thereby functions as a guardian against autoimmunity and tumor development. FAS triggers apoptosis through FADD-mediated recruitment and activation of caspase-8. In certain cells such as hepatocytes, albeit not lymphocytes, FAS-induced apoptosis requires amplification through proteolytic activation of the proapoptotic BCL-2 family member BID. Curiously, several components of the FAS signaling machinery have been implicated in nonapoptotic processes, including cellular activation, differentiation, and proliferation. This review describes current understanding of Fas-induced apoptosis signaling and proposes experimental strategies for future advances.

Introduction

The cell surface-bound receptor FAS (also called APO-1 or CD95) was originally discovered as the target of two monoclonal antibodies that trigger apoptotic cell death in certain human tumor-derived cell lines in culture or as xeno-transplants in immunodeficient mice. Cloning of the gene encoding FAS revealed that it is a member of the tumor necrosis factor receptor (TNF-R) family (Itoh et al., 1991), which also includes the receptors for TNF, TRAIL (TNF-related apoptosis-inducing ligand), and those for other members of the TNF cytokine family. Accordingly, identification of the physiological ligand for FAS, called FAS ligand (FASL or CD95L) (Suda et al., 1993), through expression cloning demonstrated that it belongs to the TNF cytokine family. The discovery that certain spontaneous mutant mouse strains that develop lymphadenopathy and SLE (systemic lupus erythematosus)-like autoimmune disease carry homozygous defects in the genes encoding FAS (*Fas*$^{lpr/lpr}$ or *Fas*$^{lprcg/lprcg}$) (Watanabe-Fukunaga et al., 1992) or FASL (*Fasl*$^{gld/gld}$) (Takahashi et al., 1994) and the realization that a large fraction of human ALPS (autoimmune lympho-proliferative syndrome) patients have heterozygous inherited mutations in the *FAS* gene (Fisher et al., 1995; Rieux-Laucat et al., 1995) demonstrated that FASL-FAS signaling plays a critical role in the control of the immune system. ALPS patients (Straus et al., 2001) as well as the FAS- or FASL-deficient mice have an abnormally increased predisposition to lymphoma development, demonstrating that FASL-FAS signaling is also critical for tumor suppression, at least within the lymphoid compartment. FASL expressed on activated T lymphocytes or natural killer (NK) cells contributes to their ability to kill target cells, such as virus-infected or damaged cells. Abnormally increased FASL-mediated killing of healthy (FAS$^+$) bystander cells has been implicated in certain immunopathological states, such as hepatitis induced by extensive T cell activation. Pharmacological modulation of the FASL-FAS signaling machinery may therefore be a useful strategy for therapeutic intervention in certain diseases, but caution is warranted because administration of agonistic FAS-specific antibodies (Ogasawara et al., 1993) or FASL (Huang et al., 1999) cause extensive hepatocyte apoptosis and fatal hepatitis in mice. Detailed understanding of FASL-FAS signaling may allow the development of more subtle intervention strategies and, interestingly, one FAS-specific antibody was shown to cure *Fasl*$^{gld/gld}$ mutant mice from their lymphadenopathy without causing liver toxicity (Ichikawa et al., 2000).

Mechanisms of FASL-FAS Signaling Induced Apoptosis

It has been argued that researchers readily observe that FAS stimulation causes apoptosis because activators of FAS (agonistic antibodies or recombinantly produced forms of FASL) have been selected for this property and that we may therefore have overly emphasized this function of FASL-FAS signaling while underestimating other activities, such as induction of cellular proliferation or differentiation (Peter et al., 2007). However, activation of FAS by its physiological ligand, FASL, has certainly been proven to trigger apoptosis (Krammer, 2000; Nagata, 1997). For example, several studies have shown that cytotoxic T cells, which express FASL in membrane-bound form (mFASL) on their surface, can kill FAS$^+$ target cells, and neutralization of FASL with specific antibodies or FAS-Fc fusion proteins proved that this killing is mediated by FASL-induced activation of FAS (Krammer, 2000; Nagata, 1997). Moreover, restimulation of already activated normal T cells or T lymphoma-derived cell lines via their TCR (T cell antigen receptor) complex causes extensive suicide or fratricide, a process called activation-induced cell death (AICD). (It has recently been proposed to rename this process "restimulation-induced cell death" [RICD] in order to distinguish it more clearly from the cell death that can occur when naive T lymphocytes are stimulated for the first time with antigen or mitogen.) Experiments with *Fas*$^{lpr/lpr}$ or *Fasl*$^{gld/gld}$ mice or the aforementioned FASL blockers

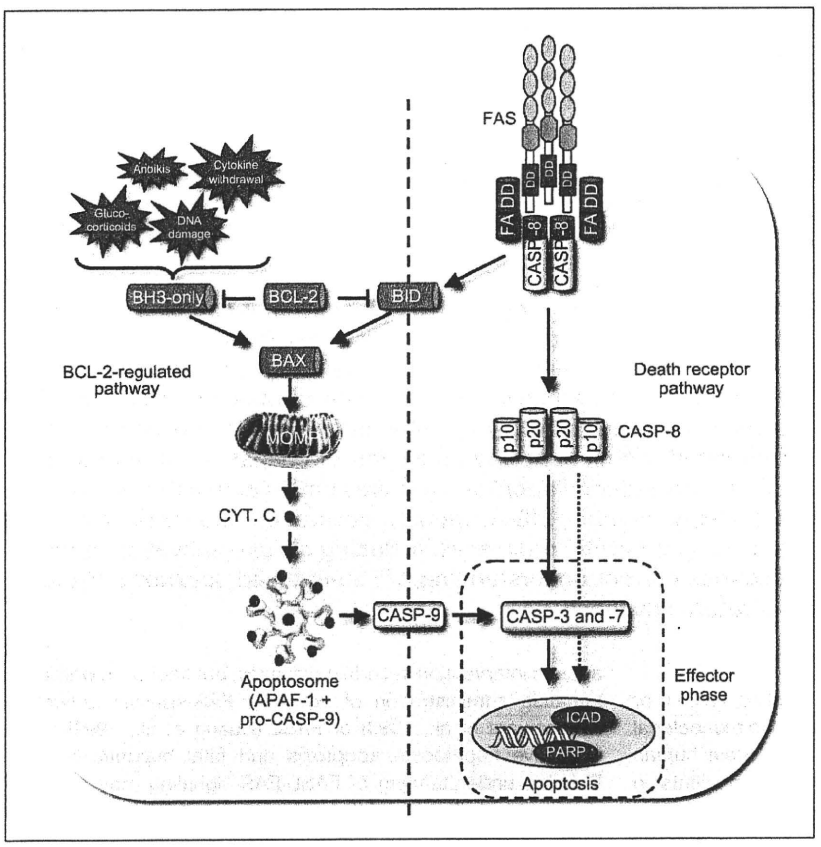

Figure 1. Death Receptor-Induced and Bcl-2-Regulated Apoptosis Signaling
This figure shows the two distinct but ultimately converging apoptosis signaling pathways in mammals. One is activated by so-called death receptors, members of the tumor necrosis factor receptor (TNF-R) family with an intracellular death domain, and requires FADD-mediated activation of caspase-8 (shown on the right). Auto-processing of caspase-8 results in a heterotetrameric form of the protein that is able to activate the zymogens of effector caspases, caspase-3 and caspase-7, eventually leading to cleavage of vital proteins within the cell, such as PARP or lamins, or activation of the DNase CAD (caspase-activated DNase) by cleavage of its inhibitor, ICAD (inhibitor of CAD). It is possible that caspase-8 may also proteolyze to a certain extent some of the classical substrates of effector caspases. The BCL-2-regulated pathway (shown on the left) is arbitrated by the complex interplay between pro- and antiapoptotic members of the BCL-2 protein family and involves mitochondrial outer membrane permeabilization (MOMP). MOMP results in release of cytochrome C from the intermembrane space of the mitochondria into the cytosol to initiate apoptosome formation resulting in APAF-1-mediated activation of the "initiator" caspase, caspase-9, further leading to proteolytic activation of the downstream effector caspases, caspase-3 and caspase-7. Abbreviations: BH3-only, BCL-2 homology domain 3 only protein; MOMP, mitochondrial outer membrane permeabilization; Cyt. C, cytochrome C; ICAD, Inhibitor of caspase activated DNase (CAD); PARP, Poly (ADP-ribose) polymerase.

showed that this apoptosis is caused (at least in part) by physiological FASL-FAS signaling (reviewed in Krammer [2000]; Nagata [1997]). It is widely believed that defects in this process underlie the lymphadenopathy and autoimmune disease that develop in mice and humans that have abnormalities in their genes encoding FAS or FASL (Krammer, 2000; Nagata, 1997).

Given that physiological FASL-FAS signaling can induce apoptosis, we first describe the mechanisms of this process, but nonapoptotic processes that are reportedly activated by FAS will also be discussed. Elegant biochemical studies have shown that ligation of FAS rapidly causes assembly of an intracellular "death-inducing signaling complex" (DISC) (Kischkel et al., 1995), which was shown to contain the aspartate-specific cysteine protease, caspase-8 (Boldin et al., 1996; Muzio et al., 1996), its adaptor/activator FADD (Boldin et al., 1995; Chinnaiyan et al., 1995), and its modulator c-FLIP (FLICE [i.e., caspase-8] inhibitory protein) (Irmler et al., 1997). The interaction between FAS and FADD requires homotypic interaction of "death domains" (DD) (Boldin et al., 1995; Chinnaiyan et al., 1995), which are present in the intracellular region of FAS also in FADD (Figure 1). The recruitment of caspase-8 by FADD is mediated (at least in part) by homotypic interaction of "death effector domains" (DED) (Boldin et al., 1996; Muzio et al., 1996), which are present in both proteins (Figure 1). Studies with gene-targeted mice and transgenic mice expressing a dominant-negative mutant of FADD (FADD-DN) or a viral enzymatic inhibitor of caspase-8 (CRMA, cytokine response modifier A) demonstrated that FADD-mediated activation of the proteolytic activity of caspase-8 is essential for FAS-induced apoptosis in many (possibly all) cell types (including lymphoid and other hemopoietic ones) both in vitro and within the whole animal (Kang et al., 2004, 2008; Newton et al., 1998; Salmena et al., 2003; Varfolomeev et al., 1998; Zhang et al., 1998). It is noteworthy that in human cells, FAS activation also causes recruitment of caspase-10 into the DISC and that in certain cell lines, caspase-10 activation was reported to contribute to apoptosis signaling. Mice do not have a gene encoding caspase-10, and because the activation and function of caspase-10 are thought to be very similar to those of caspase-8, we will not deal with caspase-10 in detail in this review. Caspase-8 activation within the DISC occurs in two steps. First, recruitment of FADD to the intracellular region of FAS promotes (via homotypic interaction of "death effector domain" [DED] recruitment) dimerization and a conformational change in caspase-8 within the DISC that allows caspase-8 to gain full enzymatic activity (Boatright et al., 2003). Second, active caspase-8 undergoes autoproteolytic processing, which allows the enzyme to leave the DISC and gain access to substrates in other cellular compartments (Boatright et al., 2003). Experiments with caspase-8-deficient (*Casp8*$^{-/-}$) mice carrying a BAC transgene encoding WT caspase-8 or a mutant of caspase-8 that has full enzymatic activity but cannot cleave itself demonstrated that autoproteolysis of caspase-8 is essential for FAS-induced apoptosis, at least in lymphoid cells and hepatocytes (Kang et al., 2008). This

indicates that upon activation, caspase-8 must leave the DISC to be able to trigger apoptosis, probably so that it can gain access to critical proteolytic substrates. Active caspase-8 can proteolytically activate downstream effector caspases, such as caspase-3 and caspase-7 (Figure 1), but (at least theoretically) this may also directly contribute to cell demolition by proteolysis of certain cellular proteins. During the later stages of apoptosis, effector caspases perform the bulk of the proteolysis of vital cellular proteins, such as structural components (e.g., lamins, gelsolin), and they can also activate certain processes that dismantle nonproteinaceaous cellular constituents (Salvesen and Dixit, 1997). For example, effector caspase-mediated cleavage of ICAD (inhibitor of caspase-activated DNase), which acts as both a chaperone and inhibitor of CAD (caspase-activated DNase), is critical for internucleosomal DNA cleavage, a hallmark of apoptosis (Salvesen and Dixit, 1997).

The c-FLIP protein, which structurally resembles caspase-8 (presence of DED but no enzymatic activity), appears to affect FAS-induced apoptosis in opposite ways depending on the extent of its expression (Figure 1). At low concentration it is thought to promote caspase-8 activation, possibly because caspase-8 binds to c-FLIP with higher affinity than to itself (i.e., in caspase-8 homodimerization). In contrast, at high concentration c-FLIP reduces the proteolytic activity of caspase-8, possibly by competing for binding to FADD, and thereby inhibits apoptosis (Boatright et al., 2003). Studies with gene-targeted mice confirmed that c-FLIP has a dual role, because its selective loss in T lymphocytes or fibroblasts accelerated their Fas-induced apoptosis (Zhang and He, 2005), although loss of c-FLIP in all tissues pheno-copied the embryonic lethality seen in *Casp8*$^{-/-}$ mice (Yeh et al., 2000), which is caused by loss of a nonapoptotic function of caspase-8 (Varfolomeev et al., 1998).

The proapoptotic BH3-only family member BID is a critical substrate of caspase-8. Its proteolysis allows the truncated BID (tBID) to translocate from the cytosol to the outer mitochondrial membrane, thereby unleashing its proapoptotic activity (Figure 1; Li et al., 1998; Luo et al., 1998). BH3-only proteins (BID, BAD, BIK [also called BLK or NBK], HRK [also called DP5], BIM [also called BOD], NOXA, Puma [also called BBC3], and BMF) form one of the two proapoptotic subgroups of the BCL-2 protein family. Their name derives from the fact that they share with each other and the BCL-2 family at large only the ~16–24 aa BH3 region (Huang and Strasser, 2000). The BH3-only proteins are essential for initiation of developmentally programmed cell death and stress-induced apoptosis and they are activated in a death stimulus- as well as cell type-specific manner (Huang and Strasser, 2000). BAX, BAK, and BOK belong to the second proapoptotic (often called the "BAX-BAK" or "multi-BH domain") subgroup of the BCL-2 family. These proteins contain three BH (BCL-2 homology) regions and although they share surprisingly extensive structural similarity to their prosurvival relatives, they are required for mitochondrial outer membrane permeabilization (MOMP) and activation of the caspase cascade in the "BCL-2-regulated" (also called "mitochondrial" or "intrinsic") apoptosis signaling pathway (Green and Kroemer, 2004). The antiapoptotic BCL-2 family members—BCL-2, BCL-XL, BCL-W, A1, and MCL-1—share with each other up to four regions of homology (BH1, 2, 3, and 4) and are essential for cell survival, functioning in a cell type-specific manner (Youle and Strasser, 2008). There are currently two models to explain the functional interactions of the three BCL-2 subgroups in apoptosis signaling. The "direct model" suggests that the BH3-only proteins bind and thereby activate BAX and/or BAK directly and that the prosurvival relatives function to bind and sequester the BH3-only proteins (Green and Kroemer, 2004). The "indirect model" proposes that in healthy cells BAX and BAK are kept in check by the prosurvival BCL-2 family members and that BH3-only proteins, when induced by apoptotic stimuli, bind with higher affinity to the prosurvival BCL-2-like proteins, thereby unleashing BAX and/or BAK (Youle and Strasser, 2008). Regardless, experiments with gene-targeted mice and biochemical studies have shown that caspase-8-mediated proteolytic activation of BID is essential for FAS-induced killing in hepatocytes (within the whole animal) (Kaufmann et al., 2007; Yin et al., 1999) and pancreatic β cells (in culture) (McKenzie et al., 2008). In contrast, BID is dispensable for Fas-induced apoptosis in lymphoid cells (both in culture and within the whole animal) and accordingly, in contrast to FAS- or FASL-deficient mice, *Bid*$^{-/-}$ mice do not develop lymphadenopathy or autoimmunity (Kaufmann et al., 2007, 2009). The reasons for this discrepancy in FAS-induced apoptosis signaling between so-called type 1 (e.g., lymphocytes) and type 2 (e.g., hepatocytes) cells are presently unclear (Scaffidi et al., 1998), but they may be due to differences in FAS aggregation or internalization or differences in the extent of caspase activation or the amount of substrates that must be proteolyzed for the cells to die (Peter et al., 2007).

Some time ago, it was proposed that FAS-induced apoptosis occurs not only when FASL-expressing killer cells engage FAS^{+} target cells, but also when cells are treated with certain chemotherapeutic drugs or γ-radiation (Debatin and Krammer, 2004). It was suggested that these cytotoxic stimuli induce FASL expression (via ceramide induction) and/or increase surface membrane deposition of Fas via a P53-dependent mechanism, both processes ultimately leading to autocrine or paracrine FASL-FAS-induced apoptosis. Studies with cells from *Fas*$^{lpr/lpr}$ mice did, however, show that γ-irradiation and chemotherapeutic drugs do not require Fas to trigger apoptosis (Newton and Strasser, 2000). Moreover, experiments with primary cells from mutant mice lacking FADD (Newton et al., 1998; Newton and Strasser, 2000; Yeh et al., 1998; Zhang et al., 1998) or caspase-8 function (Salmena et al., 2003; Varfolomeev et al., 1998) demonstrated that "death receptor" signaling in toto is not required for these pathways to apoptosis. Although we cannot rule out the possibility that the mechanisms regulating apoptosis differ markedly among distinct tumor cells, expression of dominant-negative FADD, CRMA, or c-FLIP had no impact on chemotherapeutic drug-induced killing of a collection of lymphoma-derived cell lines, demonstrating that FADD and caspase-8 are dispensable for this process in at least certain cancers (Strasser et al., 1995, 2000). We surmise that increased expression of FAS, FASL, and certain other members of these receptor and ligand families in chemotherapeutic drug-treated or γ-irradiated cells is a consequence of cellular stress. Although this process is not required for the death of these cells, it may be exploited therapeutically as illustrated by the synergistic effects of TRAIL (APO-2L, a TNF cytokine family member) and certain chemotherapeutic drugs (e.g., 5-fluoro-uracil) in the killing of certain tumor cells (Ashkenazi et al., 1999).

Collectively, these observations demonstrate that FADD-mediated recruitment and activation of caspase-8 are essential for FAS- and all death receptor-induced apoptosis and that the BH3-only protein BID is critical for this cell killing in some, albeit not all, cell types.

The Role of FASL-FAS-Induced Apoptosis in Normal as well as Pathological Killing of Target Cells

Both classical $CD8^+$ cytotoxic T cells as well as a portion of activated $CD4^+$ T cells express FASL on their surface in membrane-bound form (mFASL). Cleavage by a metallo-protease causes shedding of FASL and the resulting soluble FASL, sFASL, can still bind FAS (Tanaka et al., 1995, 1998). Studies with various forms of FASL that were produced in *E. coli* or transfected mammalian cell lines have indicated that mFASL kills target cells via FAS activation much more potently than does sFASL (Schneider et al., 1998; Suda et al., 1997; Tanaka et al., 1998). This is consistent with the notion that extensive aggregation of multiple preassembled FAS trimers and not only FASL trimer-FAS trimer interaction is required for apoptosis induction (Siegel et al., 2000). There is also some confusion in the literature based on the findings that some cultured cell lines shed mFASL-bearing vesicles into the supernatant. Although such vesicles can kill FAS^+ cells in vitro (Schneider et al., 1998), the physiological relevance of this process is currently unclear.

Comparison of T cells lacking both functional FASL and perforin ($Fasl^{gld/gld}Prf1^{-/-}$) with $Prf1^{-/-}$ T cells demonstrated that these two cell death-inducing proteins account for most killing activity of cytotoxic T cells and NK cells (Kägi et al., 1994), possibly with some additional contribution by TNF-α. Whereas FASL normally contributes to the killing of virus-infected, damaged, or excess cells, abnormally increased FASL-induced apoptosis of cells that should not be killed has been implicated as a cause of certain immuno-pathological disorders. For example, it has been shown that acute graft-versus-host (GvH) disease in mice can be prevented by combined treatment with neutralizing antibodies to FASL plus TNF-α (Hattori et al., 1998). Moreover, FASL was found to be critical for the pathological killing of hemopoietic progenitors during cytomegalovirus (CMV) infection (Mori et al., 1997). Interestingly, transfer of lymphocytes from $Fas^{lpr/lpr}$ mutant mice into congenic recipients elicits fatal GvH. This is due to the fact that Fas-deficient T cells produce abnormally high amounts of mFASL, which kill FAS^+ target cells within the host (Watanabe et al., 1995), because transfer of lymphocytes from FASL-FAS doubly deficient ($Fasl^{gld/gld}Fas^{lpr/lpr}$) mice does not cause GvH disease (Zhu et al., 2000). When the Fas^{lpr} mutation was crossed onto the NOD background, it was observed that such NOD-$Fas^{lpr/lpr}$ mice do not develop diabetes and therefore concluded that FASL-FAS signaling is critical for the pathological destruction of islet β cells in type I diabetes (Chervonsky et al., 1997). The interpretation of this finding is, however, confounded by the complication that these animals rapidly develop profound lymphadenopathy and that $Fas^{lpr/lpr}$ (and $Fasl^{gld/gld}$) mice actually become highly immunocompromised when they develop lymphadenopathy. Indeed, experiments in which islets from NOD-$Fas^{lpr/lpr}$ mice were transplanted into NOD mice demonstrated that FASL-FAS signaling played only a minor role in β cell destruction in these diabetes-prone animals (Allison and Strasser, 1998). Conversely, experiments in which diabetogenic T cells from NOD mice were injected into NOD-$Fas^{lpr/lpr}$*scid/scid* recipients (precluding excess FASL expression in the host) showed that FAS contributes to β cell destruction, at least within this context (Su et al., 2000). Analysis of perforin-deficient NOD mice revealed that as for the physiological killing of virus-infected target cells, the perforin-granzyme system plays a major role in the pathological killing of β cells in type I diabetes (Kägi et al., 1997). On the basis of all these data, we conclude that perforin plays the principal and FASL a contributory role in β cell destruction during the development of type I diabetes.

Although FASL has been widely reported to be expressed predominantly (perhaps exclusively) in antigen-stimulated T lymphocytes (both $CD8^+$ and also some $CD4^+$ T cells) and NK cells (Krammer, 2000; Mabrouk et al., 2008; Nagata, 1997), some reports indicated that in certain tissues, such as the testis, thyroid, or eye, nonhemopoietic cells can express FASL and thereby kill infiltrating T cells to establish an immune-privileged niche (Bellgrau et al., 1995). However, subsequent studies with transplantation of pancreatic islets transgenically engineered to express FASL ectopically indicated that FASL expressed on nonhemopoietic cells may not be critical to establish immune privilege (Allison et al., 1997). It has also been proposed that FASL expression on cancer cells may render them refractory to immune attack by engendering them with the ability to kill FAS^+ tumor infiltrating lymphoid and myeloid cells, but this so-called "tumor counter-attack" hypothesis has also been questioned (Restifo, 2000). Indeed, enforced expression of FASL on certain tumor cells was found to enhance rather than delay their destruction in transplant recipients (Igney et al., 2000). At least some of the confusion concerning the expression of FASL may be due to the use of unreliable reagents for its detection. The generation of gene-targeted knock-in mice (and tumors derived from them) with inducible deletion of the *Fas* (Hao et al., 2004) or *Fasl* (Mabrouk et al., 2008) genes are expected to resolve some of these controversies.

The Role of FASL-FAS-Induced Apoptosis in Lymphocyte Homeostasis

Mice lacking FAS or FASL develop progressive lymphadenopathy, which predominantly involves the so-called "unusual" ($Thy\text{-}1^+CD4^-CD8^-TCR\alpha/\beta^+B220^+$) T cells, which are thought to derive from conventional T cells that have been repeatedly activated in vivo via their TCR complex (Krammer, 2000; Nagata, 1997). These mutant mice do, however, also accumulate several-fold increases in conventional $CD4^+$ as well as $CD8^+$ T lymphocytes and B lymphocytes (Krammer, 2000; Nagata, 1997). This led to the conclusion that FASL-FAS signaling plays a critical role in the homeostasis of the lymphoid system, most likely by killing unwanted cells at one or several developmental checkpoints. During both B as well as T lymphopoiesis in primary lymphoid organs, apoptosis plays a critical role in the killing of cells that are either "useless" or "potentially dangerous" (Strasser, 2005). For example, immature lymphoid cells that failed to productively rearrange the V, (D), and J gene segments encoding one of their IG or TCR chains and therefore cannot express surface antigen receptors (BCR or TCR) are deleted as are those expressing antigen receptors that bind self-antigens with high affinity (Strasser, 2005). Because TCR

stimulation-induced apoptosis (AICD) of T lymphoma-derived cell lines requires FASL-FAS signaling (reviewed in Krammer [2000]; Nagata [1997]), it was hypothesized that FAS-induced apoptosis may be critical for the deletion of autoreactive thymocytes and immature B cells in the bone marrow. Although some studies provided evidence that FAS is essential for the deletion of thymocytes specific for so-called endogenous or experimentally applied super-antigens (antigens that are presented by antigen-presenting cells [APC] to T cells as full proteins associated with MHC molecules and not like conventional antigens as peptide fragments embedded within the MHC), this is controversial (Villunger et al., 2004). More definitive experiments with TCR or BCR transgenic mouse models confirmed that FASL and FAS are dispensable for the deletion of autoreactive thymocytes (Sidman et al., 1992) as well as autoreactive B cells developing in the bone marrow (Rubio et al., 1996), respectively. Further studies with TCR transgenic mice showed that FAS is also not required for the rapid death of naive T cells that occurs upon their transfer into hosts expressing the cognate antigen (Davey et al., 2002). In fact, studies with transgenic or gene-targeted mice that lack FADD (Newton et al., 1998) or caspase-8 function (Salmena et al., 2003) selectively in T lymphoid cells showed that death receptor-induced apoptosis signaling in toto is not required for deletion of autoreactive thymocytes. Instead the process for killing autoreactive T and B cells during their development and even in their mature state relies on the BCL-2-regulated apoptotic pathway and is initiated by the proapoptotic BH3-only protein BIM (Bouillet et al., 2002; Davey et al., 2002; Enders et al., 2003).

Programmed cell death also plays a role in the shut-down of cellular as well as humoral immune responses (Figure 2; Sprent and Tough, 2001). In the case of acute immune responses, such as infection with a nonpersisting pathogen (or injection with a degradable antigen), foreign antigen-specific T and B cells can expand several hundred-fold in numbers (Sprent and Tough, 2001). Most differentiate into effector cells (cytotoxic as well as helper T cells and antibody-producing plasma cells), which help overcome the pathogens by killing them, either directly or indirectly through cytokine-mediated activation of cells of the innate immune system. A small number of activated B and T cells differentiate into so-called "memory" cells, which are long-lived and able to respond rapidly in response to challenge with the same pathogen, thereby providing the organism with long-lasting immunity (Sprent and Tough, 2001). After pathogens have been defeated, effector cells are no longer needed and in fact are potentially dangerous, so most undergo programmed cell death (Sprent and Tough, 2001). This apoptosis restores normal cellularity in peripheral lymphoid organs, thereby making space for the development of immune responses to subsequent infectious challenges. In addition, apoptosis of activated lymphocytes minimizes the collateral damage to healthy tissues that can be caused by the immune effector molecules (e.g., inflammatory cytokines, immune complexes, perforin-granzymes) (Sprent and Tough, 2001). In the case of chronic infections with persistent antigenic challenge, the killing of activated lymphocytes is critical to achieve a state of cohabitation between the pathogen and the host, so that the numbers of pathogens are kept at an acceptable titer and at the same limiting immune activation to minimize inadvertent destruction of vital tissues (Sprent and Tough, 2001).

When FASL and FAS were discovered to be critical for TCR stimulation-induced AICD of normal cycling T lymphoblasts and transformed T lymphoma-derived cell lines (reviewed in Krammer [2000] Nagata [1997]), it was widely speculated that FASL-FAS-induced apoptosis would also prove to be essential for the death of antigen-activated T and B cells during shut-down of immune responses. For the removal of activated T cells during an acute immune response, however, this model makes little sense. The induction of FASL on T lymphoid cells undergoing AICD requires TCR stimulation, but during termination of acute immune responses, T cells die after pathogens have been expelled, a time when no antigen is present to activate the TCR. Indeed, although it was initially reported that FASL and FAS are critical for the killing of activated T cells during termination of acute immune responses (e.g., in TCR transgenic mice injected with the cognate peptide), later experiments with mice injected with a single dose of the super-antigen staphylococcus enterotoxin B (SEB) (Hildeman et al., 2002) or challenged with herpes simplex virus (HSV, causing nonpersistent infection) (Pellegrini et al., 2003) demonstrated that FAS and TNF-R1 death receptor signaling are dispensable for this process. In fact, the killing of antigen-activated T cells during termination of acute immune responses appears to be initiated by a decline in the levels of cytokines that promote their survival (e.g., IL-2, IL-7), which triggers the BCL-2-regulated apoptotic pathway predominantly through activation of the BH3-only protein BIM (Figure 2; Hildeman et al., 2002; O'Connor et al., 1998; Pellegrini et al., 2003).

In contrast to acute immune responses, pathogens and their antigens persist during chronic immune responses, thereby potentially facilitating repeated stimulation of already activated T lymphocytes through their TCR, which would then lead to FASL upregulation and their FAS-induced suicide or fratricide (Krammer, 2000; Nagata, 1997). Indeed, the first clear demonstration for a role of FAS-induced apoptosis in the shut-down of a T cell immune response came from studies in which mice were repeatedly injected with SEB (Strasser et al., 1995), thereby mimicking a chronic infection. More recently, experiments with mice infected with persistent viruses (e.g., LCMV or mouse gamma herpes virus) showed that the killing of activated T cells during the ensuing chronic immune response requires both FASL-FAS and the proapoptotic BH3-only BCL-2 family member BIM (Figure 2; Hughes et al., 2008; Hutcheson et al., 2008; Weant et al., 2008). Thus, their death appears to be caused by FASL-FAS signaling, triggered by repeated TCR stimulation, and by the BCL-2-regulated apoptotic pathway, which presumably is initiated by growth factor deprivation-induced induction of BIM.

B lymphoid cells express Fas on their surface and can be killed by treatment with FASL or agonistic FAS-specific antibodies (Krammer, 2000; Nagata, 1997) and, accordingly, FASL-FAS signaling was found to play a critical role in the control of humoral immune responses (Figure 2). The consequences of FAS activation in B cells are critically influenced by the activity of other signaling pathways. BCR crosslinking or CD40 stimulation, particularly their combination, protect B lymphocytes from FAS-induced apoptosis (Rothstein et al., 1995). This protection appears to be mediated by activation of REL-NF-κB transcription factors, which activate expression of c-FLIP (Hennino

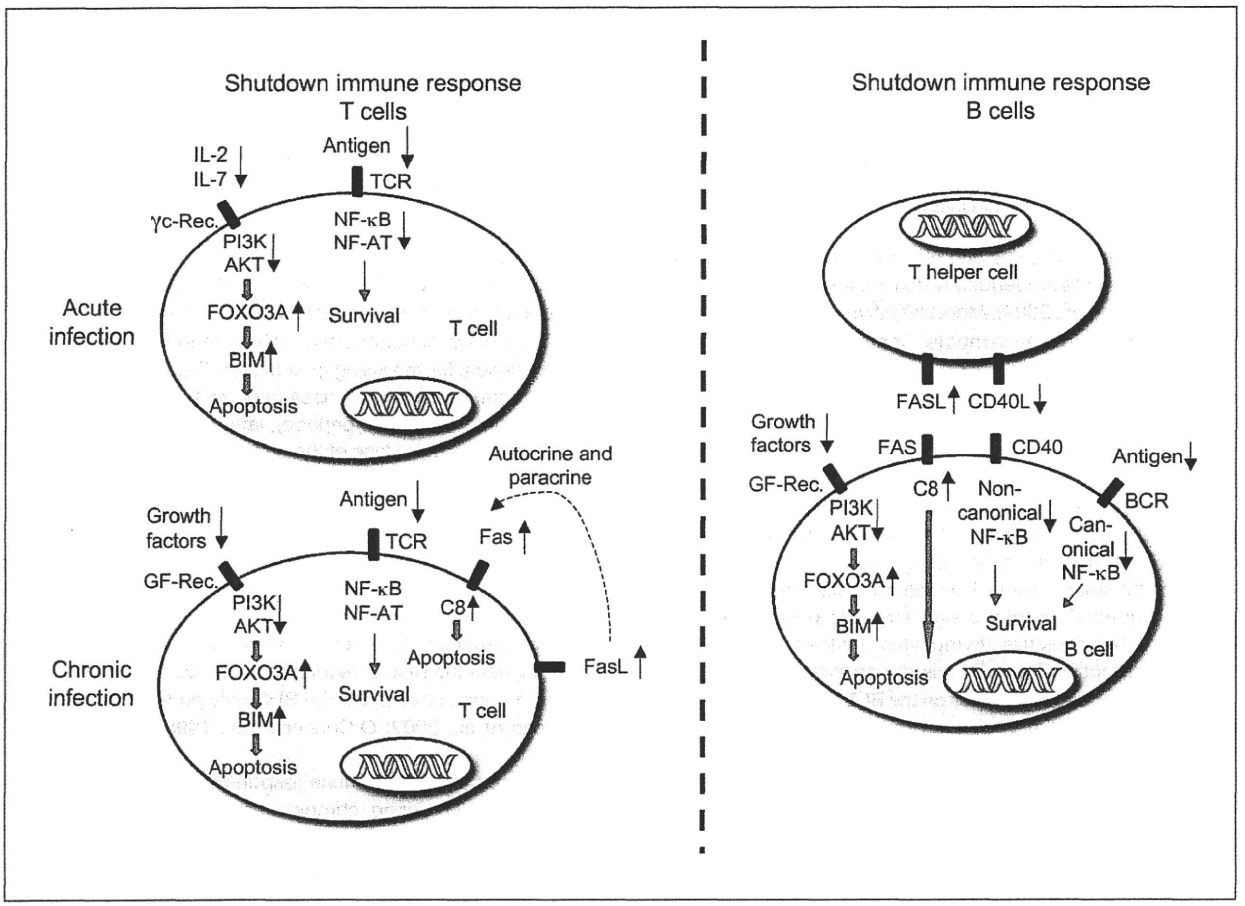

Figure 2. Fas-Mediated Death Receptor Signaling and Bcl-2-Regulated Apoptosis Signaling in the Killing of Activated T and B Lymphocytes
This figure shows the mechanisms that control FASL-FAS-induced apoptosis and BIM-dependent BCL-2-regulated apoptosis in activated T and B cells during shutdown of acute or chronic immune responses. During shutdown of an acute T cell immune response (left side, top), the reduction in the concentrations of cytokines, such as IL-2 and IL-7, leads to a reduction in PI3K and AKT. This causes activation of the transcription factor FOXO3A, which promotes transcriptional induction of the proapoptotic BH3-only protein BIM and consequently activation of the BCL-2-regulated apoptotic pathway. Furthermore, reduced antigen concentration leads to diminished TCR stimulation and consequently reduced activation of the REL-NF-κB and NF-AT transcription factors, which are known to promote expression of prosurvival proteins, such as BCL-2 or BCL-XL.
As in shutdown of acute T cell immune responses, during shutdown of a chronic T cell response (left side, bottom), the availability of growth factors is also reduced, leading to the activation of BIM and initiation of the BCL-2-regulated apoptotic pathway as described above. In addition, repeated TCR ligation triggers FASL expression on T cells leading to autocrine and/or paracrine stimulation of FAS, caspase-8 activation, activation of effector caspases, and consequently apoptosis as shown in Figure 1.
During shutdown of a B cell immune response (left side), FAS is induced on B cells and can be activated by FASL presented on T helper cells. This leads to B cell apoptosis when CD40 signaling is diminished because of reduced expression of CD40L on T helper cells, because this causes a reduction in the activity of the REL/NF-κB and NF-AT transcription factors, which normally promote expression of prosurvival proteins, such as c-FLIP. In addition, a reduction in the concentration of growth factors can lead to BIM upregulation as described above.
Abbreviations: γc Receptors, common gamma chain containing cytokine receptors (e.g., receptors for IL-2, IL-4, IL-7, IL-15); DISC, death-inducing signaling complex; GF-Rec., growth factor receptors; TCR, T cell antigen receptor; PI3K, phosphoinositide 3-kinases; BCR, B cell antigen receptor; C8, caspase 8.

et al., 2001). In fact, in combination with BCR-crosslinking and CD40 activation, FAS ligation may actually contribute to activation, proliferation, and differentiation of B cells, rather than trigger their apoptosis (Figure 2, and see below).

Germinal centers are anatomical niches within secondary lymphoid organs composed of B cells, specific $CD4^+$ T helper subsets, and follicular dendritic cells. In these locations, B cells and intrafollicular $CD4^+$ T cells recognizing the same antigenic compound are activated by interaction with each other and antigen retained on the follicular dendritic cells. This results in stimulation of B cells leading to their proliferation, hypermutation of the rearranged and expressed Ig variable region genes, and differentiation into antibody-secreting plasma cells on one hand and long-lived memory B cells on the other. During and after the germinal center reaction, activated B lymphocytes are subject to stringent selection. Only those B cells expressing high-affinity antibodies for the antigen (due to Ig V gene somatic hypermutation) can compete successfully for the limiting amount of antigen and T cell help (CD40L) and thereby gain survival signals through their BCR and CD40—low-affinity antibody-expressing B cells die by neglect. Theoretically, IGV gene hypermutation can give rise to B cells expressing BCRs specific

to self-antigens, and experiments with BCR transgenic mice showed that such autoreactive B cells are deleted by apoptosis (Shokat and Goodnow, 1995). FASL and FAS play critical roles in the control of B lymphocyte survival during the germinal center reaction (Figure 2; Krammer, 2000; Nagata, 1997). Activated B lymphocytes bearing low-affinity BCR are killed when FAS on their surface is ligated by FASL expressed on intrafollicular $CD4^+$ T cells and they fail to receive a prosurvival signal through their BCR and CD40 (Figure 2). In experimental models for deletion of autoreactive B lymphocytes within germinal centers, it was found that both FAS death receptor signaling as well as the BCL-2-regulated apoptotic pathway contribute to B cell killing (Figure 2; Rathmell et al., 1995). This is reminiscent of the finding that both of these pathways (the latter initiated by the proapoptotic BH3-only protein BIM) contribute to the killing of T cells that are chronically activated by pathogen-derived antigens or self-antigens (Hughes et al., 2008; Hutcheson et al., 2008; Weant et al., 2008). In further support of a collaboration of the FAS death receptor and the BCL-2-regulated apoptotic pathways in the deletion of autoreactive B and T cells in peripheral lymphoid organs and establishment of immunological tolerance, it was found that BCL-2 overexpression (Strasser et al., 1995) or loss of BIM (Hughes et al., 2008; Hutcheson et al., 2008; Weant et al., 2008) greatly accelerate and enhance lymphadenopathy and autoimmunity in FAS- or FASL-deficient mice. BIM was shown to play a critical role in the killing of activated B cells and IG-secreting plasma cells during shut-down of acute humoral immune responses (Fischer et al., 2007), and this BH3-only protein is probably activated by the decline in the concentration of growth factors (Figure 2).

Collectively, these results demonstrate that FAS and death receptor signaling in toto play no role in the deletion of autoreactive B or T cells during their development in primary lymphoid organs. Instead these pathways are critical, either alone or in combination with the BCL-2-regulated apoptotic pathway, for the killing of antigen-activated lymphocytes during termination of immune responses.

Unexpected Lessons from Deletion of Fas in Select Cell Types

Because FAS is expressed on a broad range of lymphoid, myeloid, and also nonhemopoietic cell types, it is not immediately clear in which cells FAS function must be lost to cause the lymphadenopathy and autoimmunity observed in FAS-deficient mice and humans (Krammer, 2000; Nagata, 1997). This important question has been addressed by generating FAS-deficient mice ($Fas^{lpr/lpr}$) that express a FAS transgene in either B and/or T cells (Fukuyama et al., 1998, 2002; Komano et al., 1999) or mice in which the sequences within the *Fas* gene that encode the death domain have been flanked by *loxP* sites and can therefore be deleted in a cell type-specific or inducible manner (via transgenic mice expressing the CRE recombinase under control of a cell type-specific or inducible promoter) (Hao et al., 2004, 2008). When interpreting data from the latter mice (and the $Fas^{-/-}$ mice [Adachi et al., 1995]), it is important to remember that cells that have undergone CRE-mediated deletion of these sequences can still express FAS (devoid of the death domain) on their surface. It has been speculated that such a truncated FAS may still be able to exert some nonapoptotic functions either directly or indirectly by so-called "reverse signaling" via FASL (Peter et al., 2007; see also below). It must also be borne in mind that several of these experiments were performed on different inbred or even mixed genetic backgrounds, so the results may not always be directly comparable, because the impact of the Fas^{lpr} and the $Fasl^{gld}$ mutations are greatly affected by genetic background. Nonetheless, these studies revealed many interesting aspects of the role of FASL-FAS signaling in the control of the normal immune system and prevention of autoimmunity (see references above). Transgenic expression of normal amounts of FAS in T cells of $Fas^{lpr/lpr}$ mice prevented lymphadenopathy, in particular the accumulation of the unusual TCR-$\alpha/\beta^+CD3^+CD4^-CD8^-B220^+$ T cells, but these animals still produced autoantibodies and developed SLE-like glomerulonephritis (Fukuyama et al., 1998). In contrast, transgenic expression of FAS on B cells protected $Fas^{lpr/lpr}$ mutant mice from SLE-like autoimmunity although abnormal accumulation of T cells, including TCR-$\alpha/\beta^+CD3^+CD4^-CD8^-B220^+$ ones, was not affected (Komano et al., 1999). Remarkably, with increasing age these mice developed a severe deficit in B cells and antibody-secreting plasma cells and this appeared to be due to the excess FASL produced by the abnormally accumulating T cells (Watanabe et al., 1995) triggering apoptosis of B lymphoid cells via the transgene-encoded FAS (Komano et al., 1999). Generation of $Fas^{lpr/lpr}$ mutant mice that lack B cells because they carry a homozygous deletion of the J_H gene locus (precluding IGH expression) showed that B cells are required for the SLE-like autoimmunity but dispensable for the T cell-associated lymphadenopathy that is caused by defects in FAS (Shlomchik et al., 1994).

Selective loss of FAS on T cells (in *Cd4-Cre* or *Ick-Cre* transgenic $Fas^{loxP/loxP}$ mice) caused progressive lymphopoenia on the C57BL/6 background albeit to a lesser extent on a (C57BL/6xMRL) F1 background (Hao et al., 2004). This cell loss was mediated by the excessive FASL produced by the FAS-deficient T lymphocytes (Watanabe et al., 1995), because it could be prevented by injection with neutralizing antibodies to FasL (Hao et al., 2004). B lymphocyte deletion in these animals was probably mediated directly, as they express FAS on their surface, but such a process cannot explain the loss of T cells, since they lack FAS. Their progressive disappearance may be due to an indirect mechanism, which involves FASL-mediated killing of FAS^+ cells that deliver critical survival signals to T lymphocytes. B lymphocytes account for some, albeit clearly not all, of these survival signals, because T cell lymphadenopathy with $CD4^+$, $CD8^+$, as well as the unusual TCR-$\alpha/\beta^+CD3^+CD4^-CD8^-B220^+$ T cells is substantially diminished (although not abrogated) in B cell-deficient $Fas^{lpr/lpr}$ mutant mice compared to control $Fas^{lpr/lpr}$ animals (Shlomchik et al., 1994).

Loss of FAS on B cells or on both B cells plus T cells (in *Cd19-Cre* transgenic or *Cd19-Cre-Cd4-Cre* bitransgenic $Fas^{loxP/loxP}$ mice) elicited lymphadenopathy, hypergammaglobulinemia, and autoantibody production (Hao et al., 2004, 2008). All of these abnormalities developed in these animals, however, to a considerably lower extent and more slowly compared to animals with loss of FAS in all tissues or in all hemopoietic cells (Mx-Cre transgenic $Fas^{loxP/loxP}$ mice injected with poly-IC). Interestingly, specific loss of FAS-mediated apoptosis in dendritic cells (with